EFFECTS OF ENVIRONMENTS ON THE SURFACE WAVE CHARACTERISTICS OF A DIELECTRIC-COATED CONDUCTOR—PART III

GLORY JOHN, R. CHATTERJEE AND S. K. CHATTERJEE

Department of Electrical Communication Engineering, Indian Institute of Science, Bangalore 560012

Received on November 19, 1975

ABSTRACT

The surface wave characteristics of a circular cylindrical conductor coated with stratified dielectrics have been theoretically studied. Six different profiles $\epsilon(\rho)$ *of dielectric constant in the* ρ*-direction, viz., square, fourth power, exponential etc. have been considered. The results of analysis indicate greater concentration of surface wave field within the dielectric media when the conductor is coated with two concentric radially stratified dielectrics satisfying square-law and fourth-power-law profiles. The attenuation constant is also less compared with that of a conductor coated with homogeneous dielectrics.*

Key words : Environmental effect, surface wave characteristics.

1. INTRODUCTION

RECENT reports [1, 2, 3] on the surface wave characteristics of a dielectric coated conductor immersed in an external dielectric medium show that

(i) the dielectric constant of the environmental medium has significant influence on the characteristics of a surface wave structure,

(ii) the surface wave characteristics depend on the ratio of the dielectric constants and also on the loss tangents of the inner and outer dielectric media,

(iii) the surfacewave tends to become more strongly bound as the anisotropy factor $(\epsilon_z/\epsilon_\rho)$ is increased, and,

(iv) under certain conditions of the relative dielectric constants and loss of the two dielectric media, the surface wave condition is not satisfied.

The above conclusions were arrived by analysing the case of a single homogeneous dielectric-coated conductor. The object of the present paper is to present the results of theoretical analysis of the effects of stratification of dielectric constant in the radial direction of dielectric coating when the surface wave structure consists of a conductor coated concentrically with two dielectrics and immersed in a dielectric medium which is infinitely extended.

2. WAVE EQUATIONS

The vector wave equations in different media (Fig. 1) are

Med. 1 ($r_1 \leq \rho \leq r_2$)

$$\nabla^2 E + k_1 E = 0. \tag{1}$$

3. DIELECTRIC CONSTANT PROFILES

The dielectric constant variation in the ρ-direction is considered as

$$\epsilon_2(\rho) = \epsilon_1 [1 - f(d\rho')] \tag{4}$$

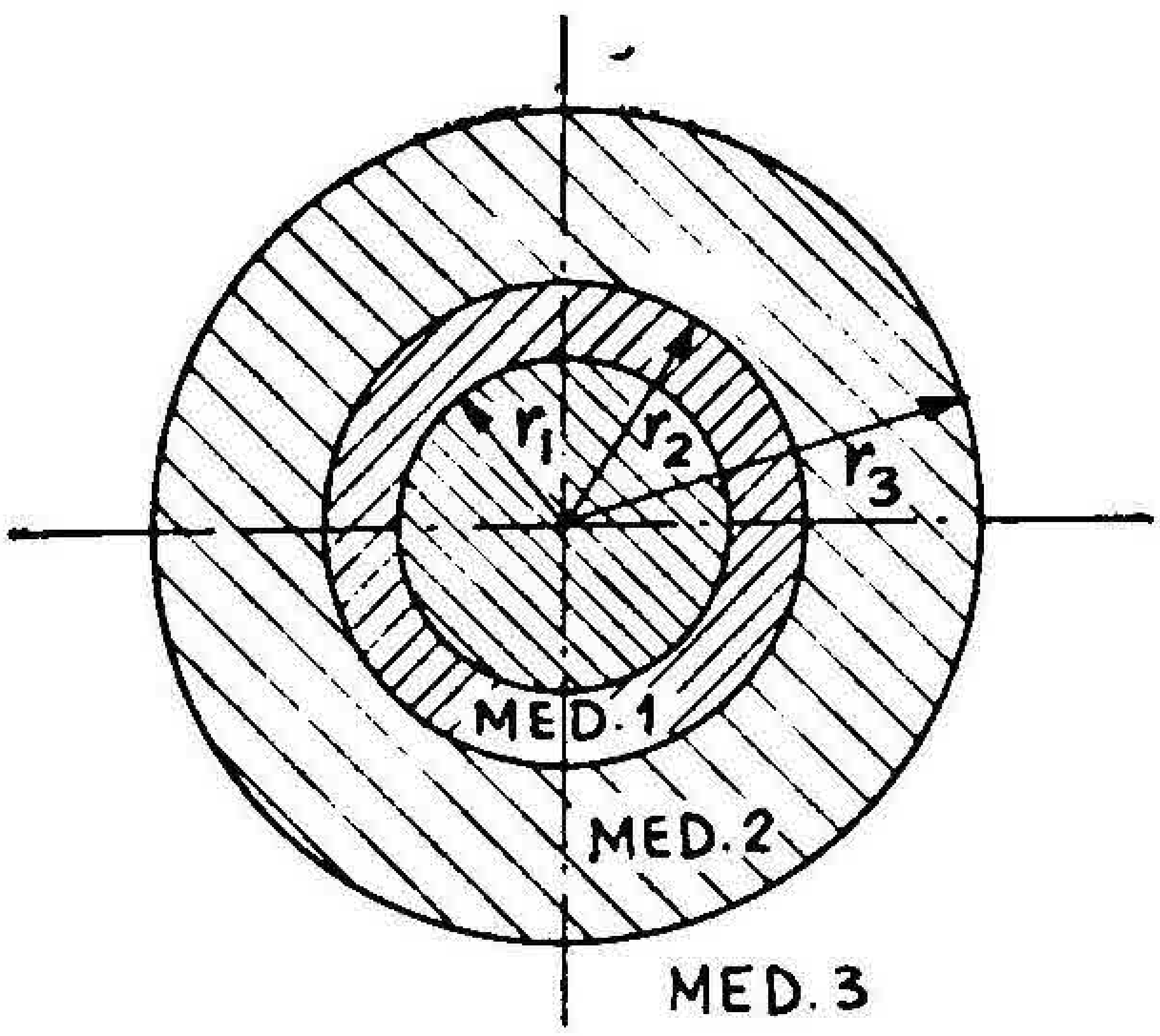

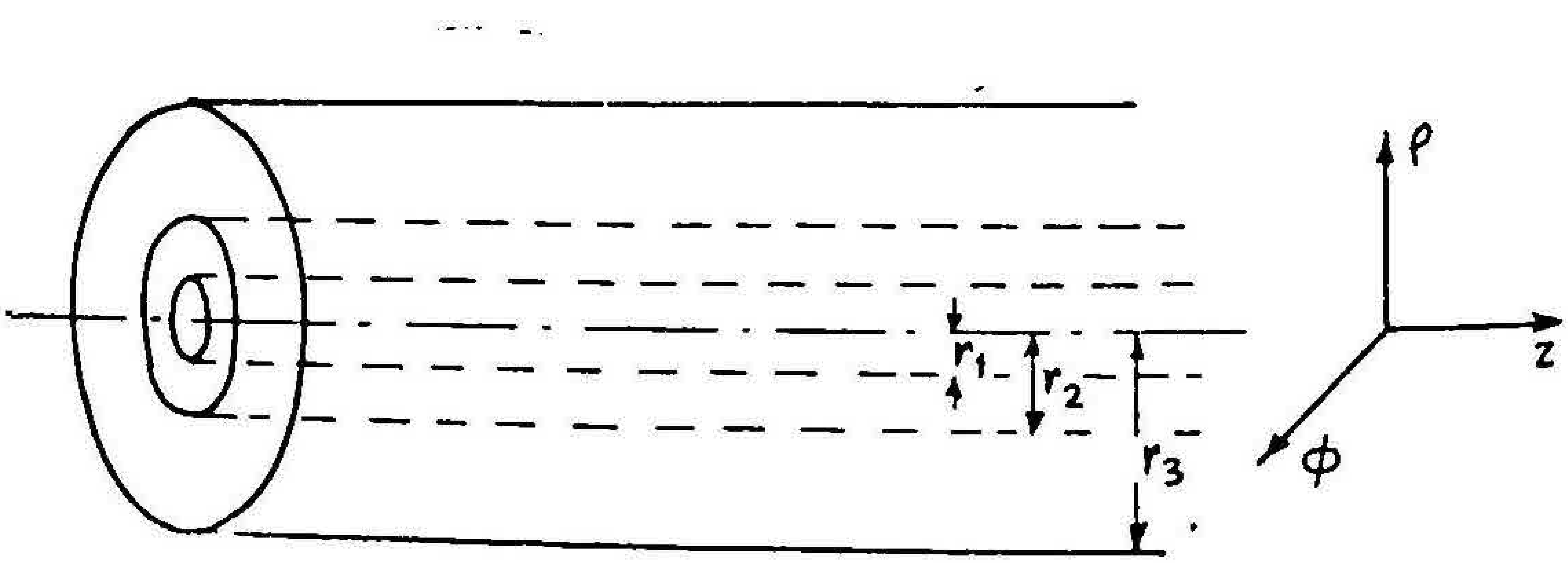

FIG. 1. Dielectric-coated conductor, coated with a graded dielectric-coordinate system Med. 1: ϵ_1, μ_0; Med. 2: $\epsilon_2(\rho)$, μ_0; Med. 3: ϵ_3, μ_0.

Med. 2 ($r_2 \leq \rho \leq r_3$) (see Appendix A. 1)

$$\nabla^2 E + \nabla \left[E \cdot \frac{\nabla \epsilon_2(\rho)}{\epsilon_2(\rho)} \right] + k_0^2 \epsilon_2(\rho) E = 0 \tag{2}$$

which can be simplified as

$$\nabla^2 E + k_0^2 \epsilon_2(\rho) E = 0 \tag{2 a}$$

by assuming that $\epsilon_2(\rho)$ is a very slowly varying function in which case the gradient term $\nabla \left[E \cdot \frac{\nabla \epsilon_2(\rho)}{\epsilon_2(\rho)} \right]$ can be ignored. It may, however, be noted that the approximation is not valid in the neighbourhood of the surface $\epsilon_2(\rho) = 0$ (see Appendix A.2)

Med. 3 ($\rho \geqslant r_3$)

$$\triangle^2 E + k_3^2 E = 0 \tag{3}$$

where

$$k_0^2 = w^2 \mu_0 \epsilon_0, \; k_1^2 = k_0^2 \epsilon_1 \quad \text{and} \quad k_3^2 = k_0^2 \epsilon_3. \tag{3 a}$$

where

$\rho' = \rho - r_2$ and $f(d\rho')$ is an analytic, monotonically increasing function of ρ satisfying the following conditions

$$f(d\rho') = 0 \quad \text{at} \quad \rho = r_1 \tag{4 a}$$

and

$$0 < [f(d\rho'), f'(d\rho')] < 1 \text{ for } r_2 \leqslant \rho \leqslant r^4 \tag{4 b}$$

where f' represents the first derivative of f with respect to ρ and d is a measure of inhomogeneity which is zero for a homogeneous dielectric medium.

The following dielectric constant profiles (*see* Figs. 2, 3) have been considered.

$$\begin{aligned}
&\text{(i)} \quad \epsilon_2(\rho) = \epsilon_1 [1 - d^2 (\rho - r_2)^2] \\
&\text{(ii)} \quad \epsilon_2(\rho) = \epsilon_1 [1 - d^4 (\rho - r_2)^4] \\
&\text{(iii)} \quad \epsilon_2(\rho) = \epsilon_1 [1 - d^2 (\rho - r_2)^2 - d^4 (\rho - r_2)^4] \\
&\text{(iv)} \quad \epsilon_2(\rho) = \epsilon_1 \operatorname{sech} d (\rho - r_2) \\
&\text{(v)} \quad \epsilon_2(\rho) = \epsilon_1 \operatorname{sech}^2 d (\rho - r_2), \text{ and} \\
&\text{(vi)} \quad \epsilon_2(\rho) = \epsilon_1 \exp [- d (\rho - r_2)].
\end{aligned} \tag{5}$$

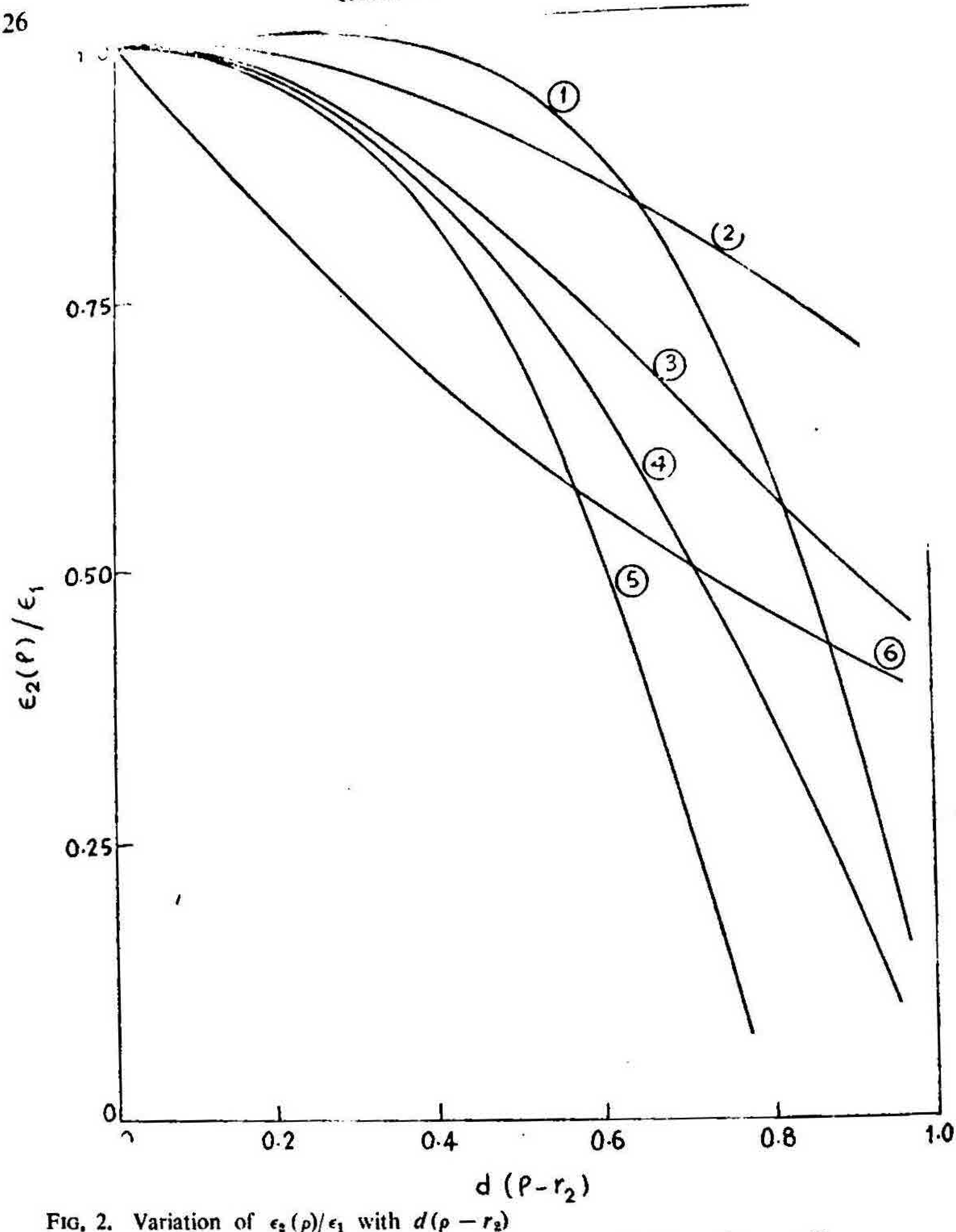

FIG. 2. Variation of $\epsilon_2(\rho)/\epsilon_1$ with $d(\rho - r_2)$

(1) $1 - d_4(\rho - r_2)^4$
(2) sech $d(\rho - r_2)$
(3) $\text{sech}^2 d(\rho - r_2)$
(4) $1 - d^2(\rho - r_2)^2$
(5) $1 - d^2(\rho - r_2)^2 - d^4(\rho - r_2)^4$
(6) $\exp[-d(\rho - r_2)]$.

The range of $d(\rho - r_2)$ considered in computing the variation of ϵ_2 as $f(\rho')$ in Fig. 2 is $0 \leq d(\rho - r_2) \leq 0.2$. Since all the six profiles vary very little over this range, only this range has been considered in the analysis, so that the approximation made in simplifying equation (2) equation (2 *a*) is valid.

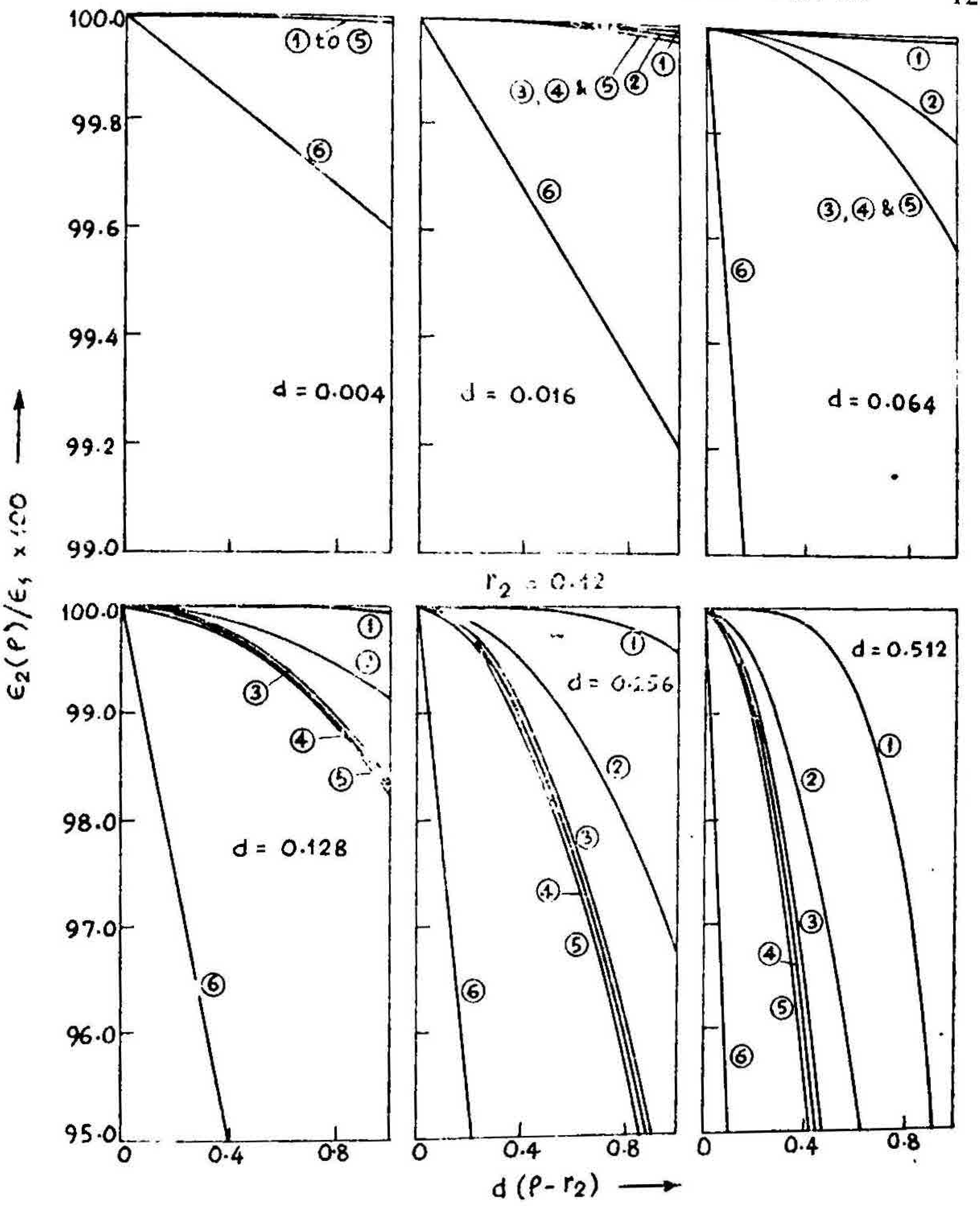

FIG. 3. Variation of $\epsilon_2(\rho)/\epsilon_1$ with $d(\rho - r_2)$
(1) $1 - d^4(\rho - r_2)^4$
(2) $\operatorname{sech} d(\rho - r_2)$
(3) $\operatorname{sech}^2 d(\rho - r_2)$
(4) $1 - d^2(\rho - r_2)^2$
(5) $1 - d^2(\rho - r_2)^2 - d^4(\rho - r_2)^4$
(6) $\exp[-d(\rho - r_2)]$.

4. FIELD COMPONENTS

The solution of wave equations in respective media yield the following field components when the mode of excitation is E_0. Med. 1 ($r_1 \leqslant \rho \leqslant r_2$)

$$E_{z1} = [A_1 J_0(a_1\rho) + A_2 Y_0(a, \rho)]\, e^{j(\omega t - \beta z)}$$

$$E_{\rho 1} = \frac{j\beta}{a_1}\left[A_1 J_1(a_1\rho) + A_2 Y_1(a, \rho)\right] e^{j(wt-\beta z)}$$

$$H_{\phi 1} = \frac{j\omega\, \epsilon_0 \epsilon_1}{a_1}\left[A_1 J_1(a_1\rho) + A_2 Y_1(a, \rho)\right] e^{j(wt-\beta z)} \tag{6}$$

Med. 2 ($r_2 \leq \rho \leq r^3$)

$$E_z{}^2 = \left[C_1 S_1(\rho) + C_2 S_2(\rho)\right] e^{j(wt-\beta z)}$$

$$E_{\rho 2} = \frac{-j\beta}{a_2{}^2(\rho)}\left[C_1 S_3(\rho) + C_2 S_4(\rho)\right] e^{j(wt-\beta z)}$$

$$H_{\phi 2} = \frac{-j\omega\, \epsilon_0 \epsilon_2(\rho)}{a_2{}^2(\rho)}\left[C_1 S_3(\rho) + C_2 S_4(\rho)\right] e^{j(wt-\beta z)} \tag{7}$$

Med. 3 ($\rho \geqslant r_3$)

$$E_{z3} = D H_0{}^{(1)}(j a_3 \rho)\, e^{j(wt-\beta z)}$$

$$E_{\rho 3} = \frac{\beta}{a_3} D H_1{}^{(1)}(j a_3 \rho)\, e^{j(wt-\beta z)}$$

$$H_{\phi 3} = \frac{\omega\epsilon_0\epsilon_3}{a_3} D H_1{}^{(1)}(j a_3 \rho)\, e^{j(wt-\beta z)} \tag{8}$$

where

$$a_1{}^2 = k_1{}^2 - \beta^2,\ a_2{}^2 = k_0{}^2\, \epsilon_2(\rho) - \beta^2,\ a_3{}^2 = \beta^2 - k_3{}^2 \tag{8 a}$$

and $S_1(\rho)$ and $S_2(\rho)$ are the two independent solutions of equation (2 *a*) and are expressed (see Apeendix A.3) as

$$S_1(\rho) = \sum_{n=0}^{\infty} c_n (b\rho)^n$$

$$S_2(\rho) = \sum_{n=0}^{\infty} d_n (b\rho)^n + \log(b\rho)\, .\, S_1(\rho) \tag{8 b}$$

$S_3(\rho)$ and $S_4(\rho)$ are expressed as derivatives of $S_1(\rho)$ and $S_2(\rho)$ respectively

$$S_3(\rho) = \frac{\partial}{\partial\rho}\left[S_1(\rho)\right]$$

$$S_4(\rho) = \frac{\partial}{\partial\rho}\left[S_2(\rho)\right] \tag{8 c}$$

where (see Appendix A. 3.2) the coefficients c_n and d_n and b depend on the physical parameters of the surface wave structure such as the radii, the dielectric constants of the coated media and the inhomogeneity factor, d.

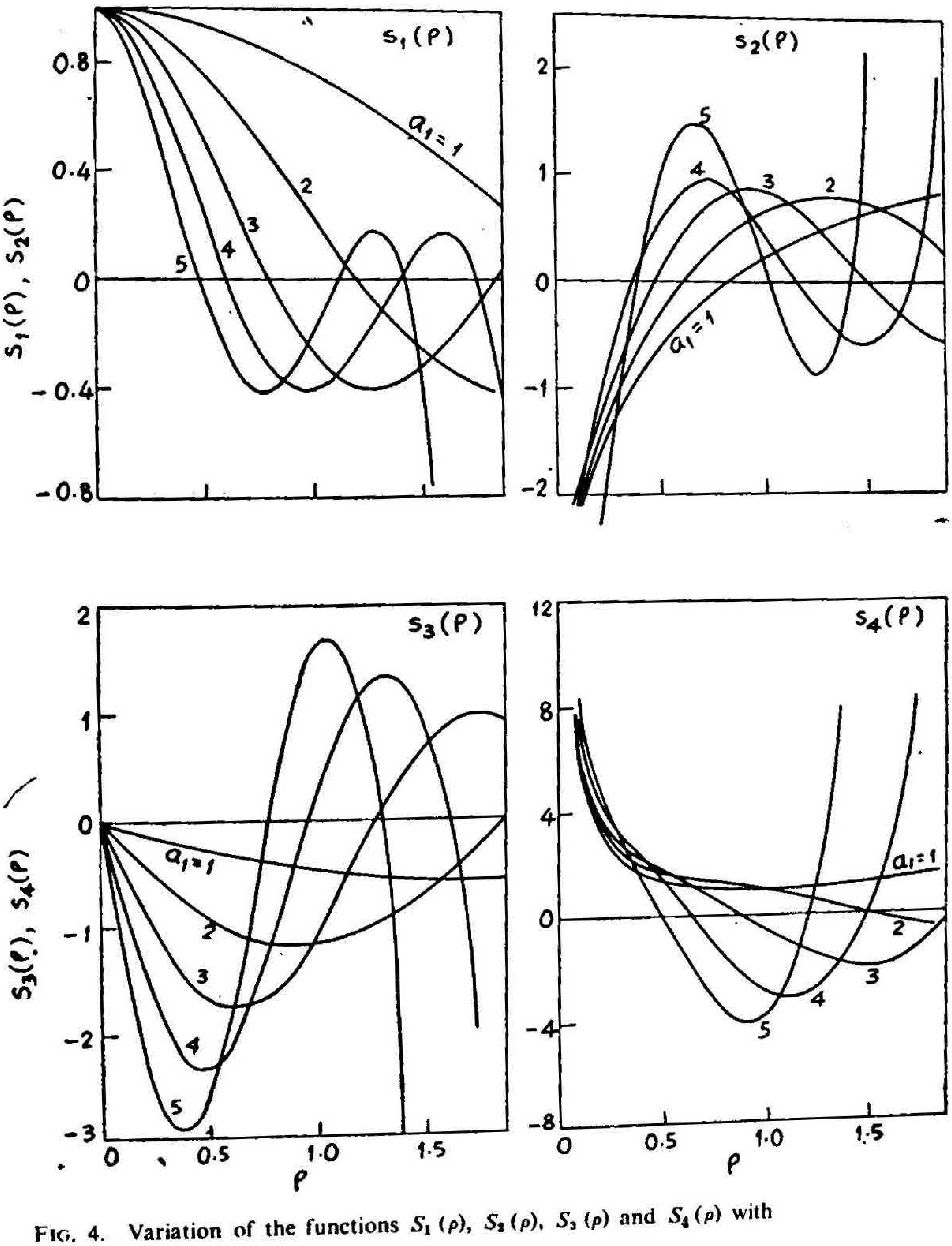

FIG. 4. Variation of the functions $S_1(\rho)$, $S_2(\rho)$, $S_3(\rho)$ and $S_4(\rho)$ with

Profile : $\frac{\epsilon_2(\rho)}{\epsilon_1} = 1 - d^2(\rho - r_2)^2$

$r_2 = 0 \cdot 12$ cm; $d = 0 \cdot 2$ cm^{-1}.

The variation of S_1, S_2, S_3 and S_4 as function of ρ for different ϵ-profiles are shown in figures 4 to 7 for values of $d = 0.2$ and 0.6.

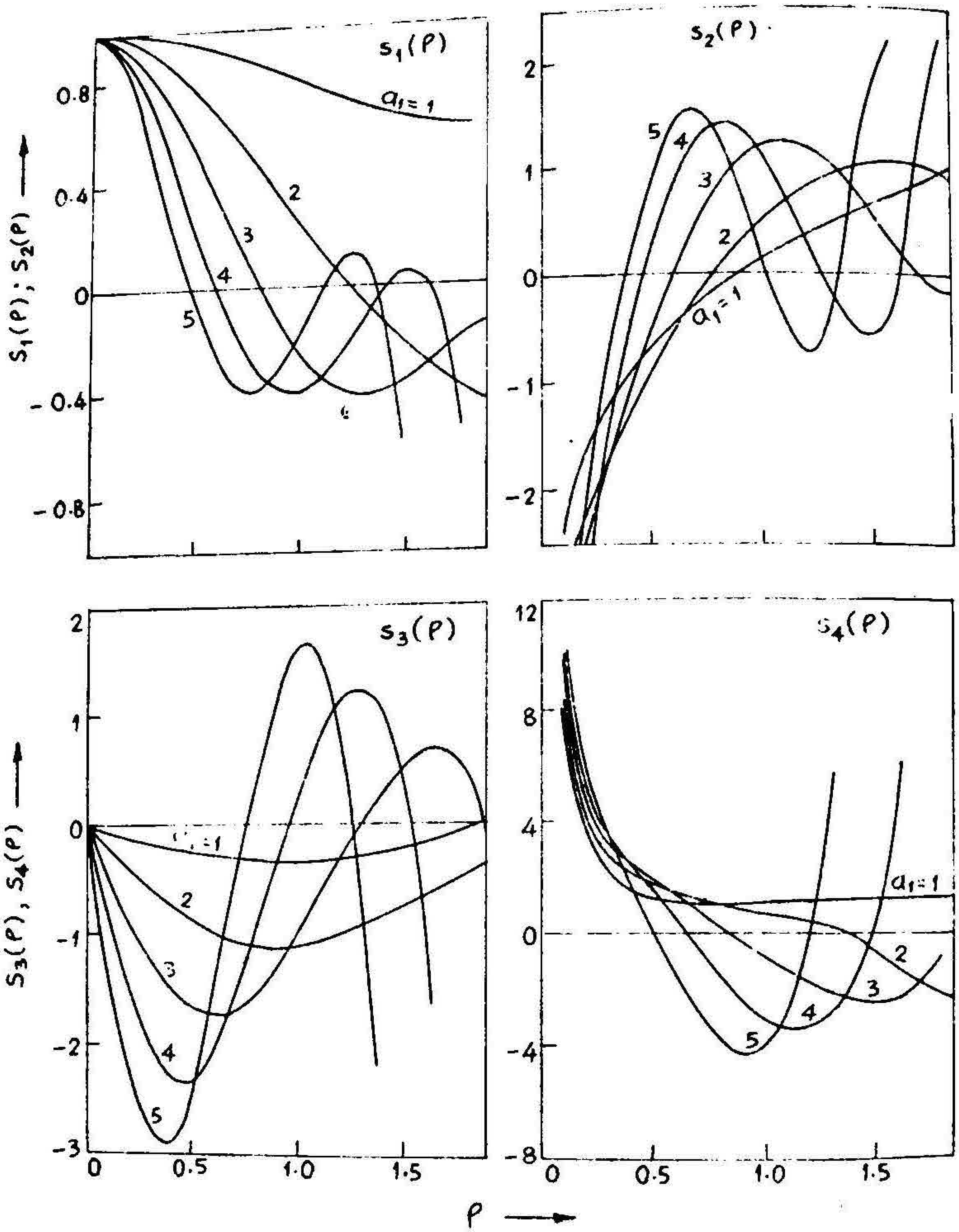

FIG. 5. Variation of the functions $S_1(\rho)$, $S_2(\rho)$, $S_3(\rho)$ and $S_4(\rho)$ with

Profile : $\dfrac{\epsilon_2(\rho)}{\epsilon_1} = \operatorname{sech} d(\rho - r_2)$

$r_2 = 0{\cdot}12$ cm, $\quad d = 0{\cdot}2\ \mathrm{cm}^{-1}$

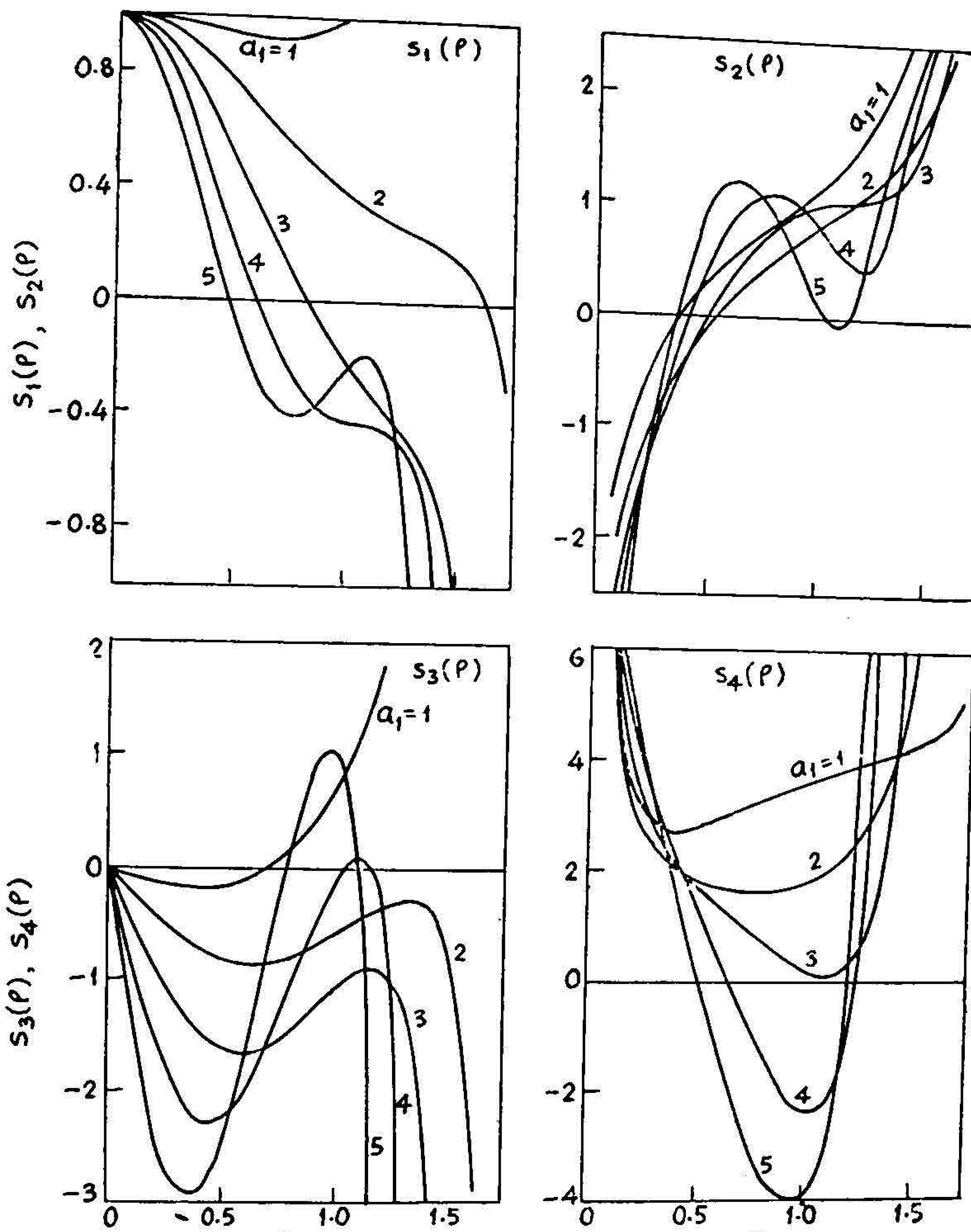

FIG. 6. Variation of the functions $S_1(\rho)$, $S_2(\rho)$, $S_3(\rho)$ and $S_4(\rho)$ with ρ

Profile : $\dfrac{\epsilon_2(\rho)}{\epsilon_1} = 1 - d^2(\rho - r_2)^2$

$r_2 = 0 \cdot 12$ cm, $d = 0 \cdot 6$ cm^{-1}.

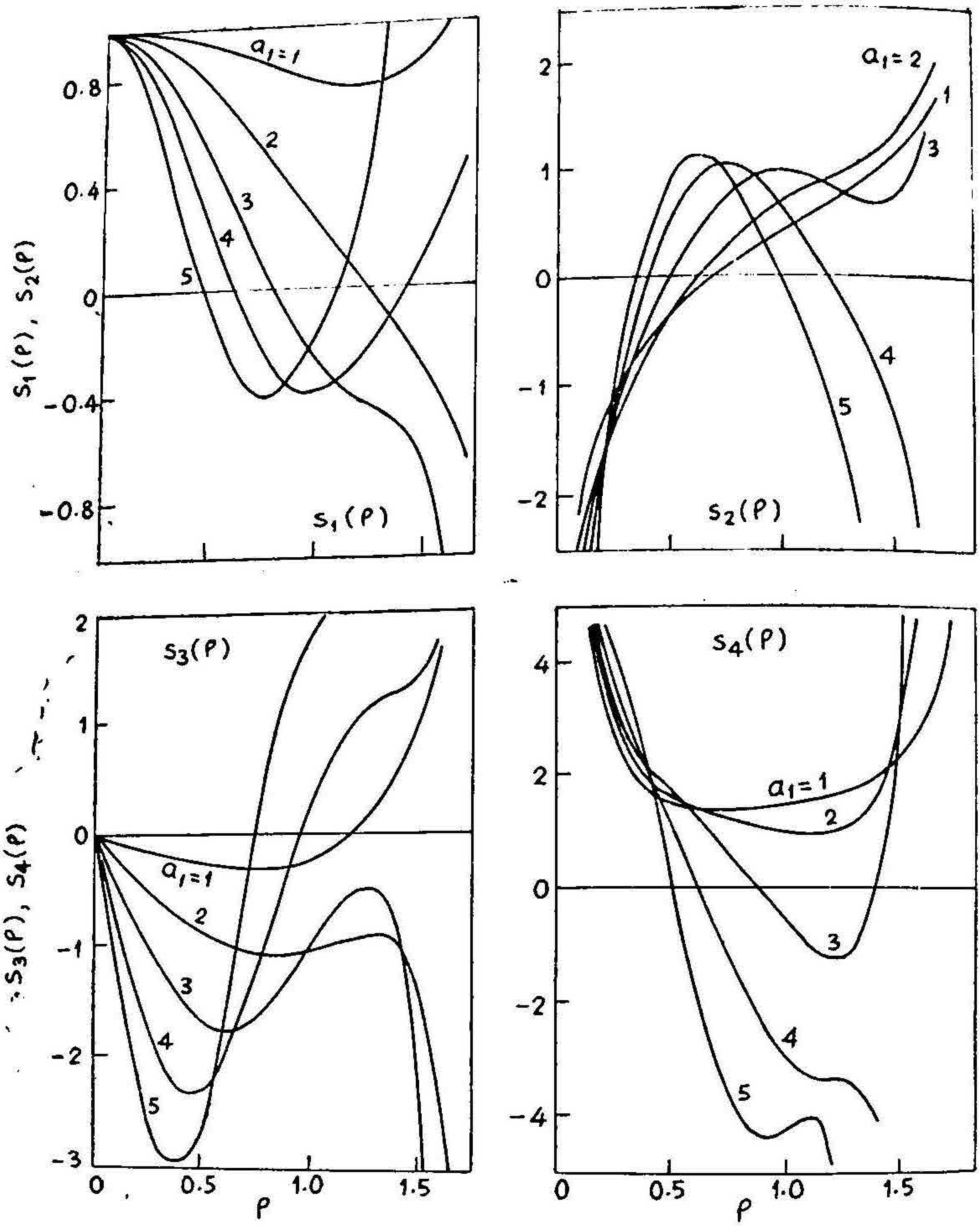

FIG. 7. Variation of the functions $S_1(\rho)$, $S_2(\rho)$, $S_3(\rho)$ and $S_4(\rho)$ with

Profile : $\frac{\epsilon_2(\rho)}{\epsilon_1} = 1 - d^4(\rho - r_2)^4$

$r_2 = 0 \cdot 12$ cm; $d = 0 \cdot 6\ \mathrm{cm}^{-1}$.

6. Characteristic Equation

By using the continuity of E_z and H_ϕ at $\rho = r_1$, r_2 and r_3 and using appropriate field components, the following equations are obtained.

(i) $A_1 J_0(a_1 r_1) + A_2 Y_0(a_1 r_1) = 0$

(ii) $A_1 J_0(a_1 r_2) + A_2 Y_0(a_1 r_2) - C_1 S_1(r_2) - C_2 S_2(r_2) = 0$

(iii) $\frac{\epsilon_1}{a_1}[A_1 J_1(a_1 r_2) + A_2 Y_1(a_1 r_2)] +$

$$X(r_2)[C_1 S_3(r_2) + C_2 S_4(r_2)] = 0$$

(iv) $C_1 S_1(r_3) + C_2 S_2(r_3) - D H_0^{(2)}(j a_3 r_3) = 0$

(v) $j X(r_3)[C_1 S_3(r_3) + C_2 S_4(r_3)] + \frac{\epsilon_3}{a_3} D H_1^{(1)}(j a_3 r_3) = 0$ (9)

where

$$X(\rho) = \frac{\epsilon_2(\rho)}{a_2^2(\rho)} \quad (\rho = r_2, r_3). \tag{9 a}$$

The above equations lead to the following determinantal equation:

$$\begin{vmatrix} J_0(a_1 r_1) & Y_0(a_1 r_1) & 0 & 0 & 0 \\ J_0(a_1 r_2) & Y_0(a_1 r_2) & -S_1(r_2) & -S_2(r_2) & 0 \\ \frac{\epsilon_1}{a_1} J_1(a_1 r_1) & \frac{\epsilon_1}{a_1} Y_1(a_1 r_2) & X(r_2) S_3(r_2) & X(r_2) S_4(r_2) & 0 \\ 0 & 0 & S_1(r_3) & S_2(r_3) & -H_0^{(1)}(j a_3 r_3) \\ 0 & 0 & j X(r_3) S_3(r_3) & j X(r_3) S_4(r_3) & \frac{\epsilon_3}{a_3} H_1^{(1)}(j a_3 r_3) \end{vmatrix} = 0 \tag{10}$$

which reduces to

$$\left[\frac{\epsilon_3}{a_3} K_1(a_3 r_3) S_2(r_3) - X(r_3) K_0(a_3 r_3) S_4(r_3)\right]$$

$$\times \left[X(r_2) S_3(r_2) F_{00}(a_1 r_2) + \frac{\epsilon_1}{a_1} S_1(r_2) F_{10}(a_1 r_2)\right]$$

$$- \left[\frac{\epsilon_3}{a_3} K_1 (a_3 r_3) \; S_1 (r_3) - X (r_3) K_0 (a_3 r_3) S_3 (r_3) \right]$$
$$\times \left[X (r_2) S_4 (r_2) F_{00} (a_1 r_2) + \frac{\epsilon_1}{a_1} S_2 (r_2) F_{10} (a_1 r_2) \right] = 0 \qquad (11)$$

where

$$H_0^{(1)} (j a_3 r_3) = - \frac{2}{\pi} j K_0 (a_3 r_3)$$
$$H_1^{(1)} (j a_3 r_3) = - \frac{2}{\pi} K_1 (a_3 r_3) \qquad (11\,a)$$

and the functions $F_{00} (a_1 \rho)$ and $F_{10} (a_1 \rho)$ are given by

$$F_{rs} (a_1 \rho) = J_r (a_1 \rho) Y_s (a_1 r_1) - J_s (a_1 r_1) Y_r (a_1 \rho). \qquad (11\,b)$$

7. SOLUTION OF THE CHARACTERISTIC EQUATION

The characteristic equation (11) has been solved with the help of the following two relations

$$a_1^2 + a_3^2 = k_0^2 (\epsilon_1 - \epsilon_3)$$

and

$$a_2^2 + a_3^2 = k_0^2 [\epsilon_2 (\rho) - \epsilon_3].$$

The solution yields the radial propagation constants from which other surface wave characteristics are calculated.

8. SURFACE WAVE CHARACTERISTICS

The numerical calculations have been made at $f = 9{\cdot}375$ GHz for $\epsilon_1 = 5{\cdot}0$, $\epsilon_0 = 8{\cdot}854 \times 10^{-14}$ farads/cm and $\mu_0 = 4\pi \times 10^{-9}$ henry/cm.

8.1. *Radial Propagation Constants*

The variation of a_1 and a_3 with ϵ_3, d and r_3/r_2 has been computed for different profiles. The variation for square-law profile is shown in Figs. 8 and 9. It is found that

(i) the radial propagation constant a_1 decreases with increasing ϵ_3 and r_3/r_2.

(ii) a_1 increases gradually with d.

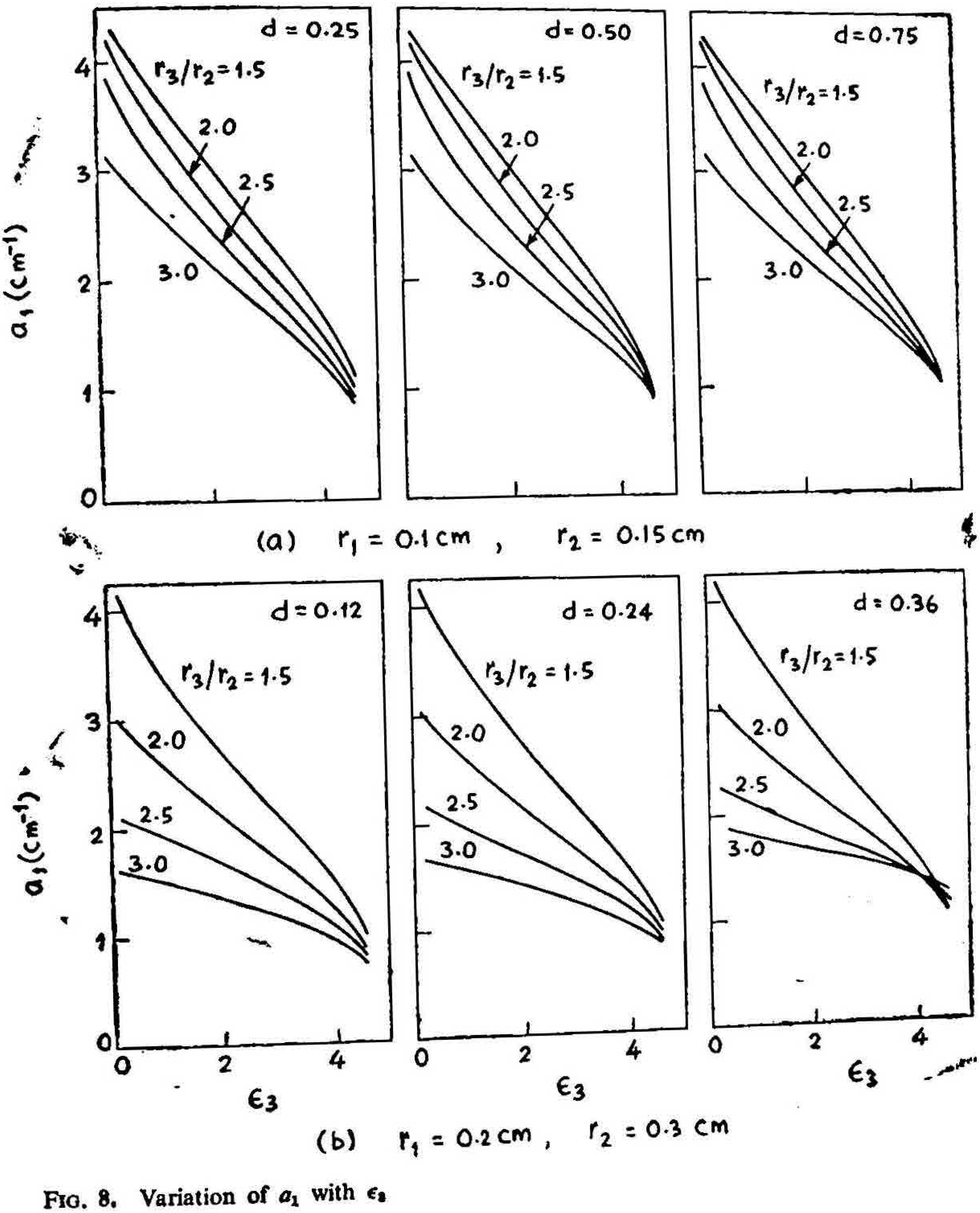

FIG. 8. Variation of a_1 with ϵ_3

Profile : $\dfrac{\epsilon_2(\rho)}{\epsilon_1} = 1 - d^2(\rho - r_2)^2$

(*a*) — $r_1 = 0{\cdot}1$ cm, $r_2 = 0{\cdot}15$ cm.

(*b*) $r_1 = 0{\cdot}2$ cm, $r_2 = 0{\cdot}3$ cm.

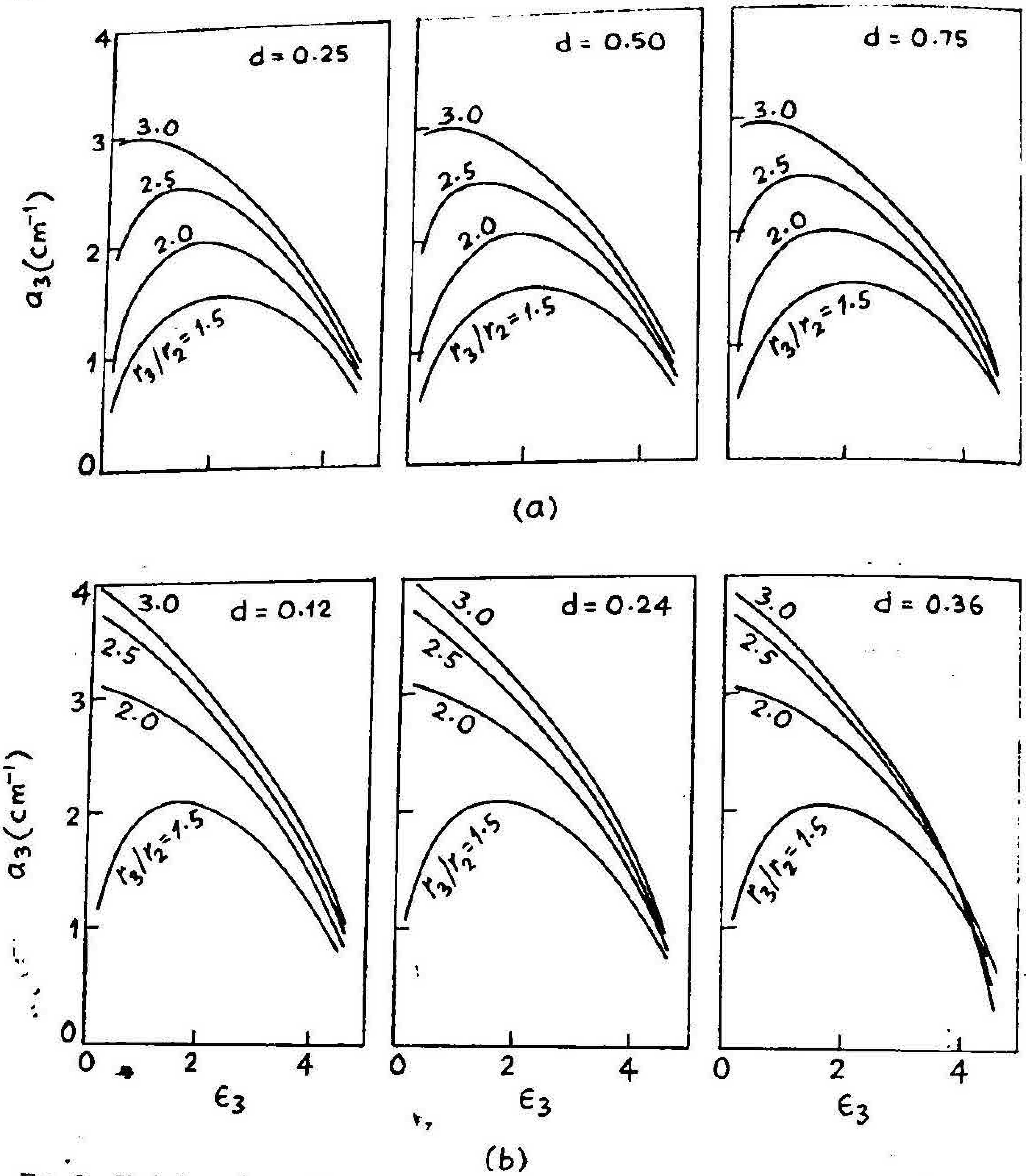

FIG. 9. Variation of a_3 with ϵ_3

Profile : $\frac{\epsilon_3(\rho)}{\epsilon_1} = 1 - d^2(\rho - r_2)^2$

(*a*) $r_1 = 0 \cdot 1$ cm, $r_2 = 0 \cdot 15$ cm.

(*b*) $r_1 = 0 \cdot 2$ cm, $r_2 = 0 \cdot 3$ cm.

(iii) a_3 increases for smaller values of r_3/r_2 and then decreases after a certain value of $\epsilon_3 \left(\simeq \frac{\epsilon_1}{2} \right)$

(iv) a_3 decreases with ϵ_3 for larger values of r_3/r_2 and decreases gradually with d when $\epsilon_3 \simeq \epsilon_1$.

The calculation of radial constant $a_2(\rho)$ for $\epsilon_3 = 0{\cdot}2$, $1{\cdot}0$ and $3{\cdot}0$, $\epsilon_1 = 5{\cdot}0$, $r_1 = 0{\cdot}1$ cm $r_2 = 0{\cdot}15$ cm, $d = 0{\cdot}3$ cm^{-1} and for a fourth order profile shows that,

(i) $a_2(\rho)$ does not change much with ρ;

(ii) $a_2(\rho)$ has a value equal to that of a_1 at $= r_2$ and decreases very slowly as ρ increases.

(iii) $a_2(\rho)$ decreases with ϵ_3 and r_3/r_2.

8.2. *Phase Constant*

The calculation of the axial phase constant β by using the relaton

$$\beta = (a_3^2 + k_3^2)^{1/2} = (k_1^2 - a_1^2)^{1/2}$$
$$= [k_0^2 \epsilon_2(\rho) - a_2^2(\rho)]^{1/2} \tag{12}$$

shows that (Fig. 10), for sech $(d\rho)$ — profile,

(i) β increases and tends to attain a constant value as ϵ_3 and r_3/r_2 increases

(ii) β increases with d.

It may be noted that β is constant in medium 2 unlike $a_2(\rho)$. The behaviour of β for square-law profile is found to be of the same nature as that of the sech $(d\rho)$ profile.

8.3. *Phase Velocity*

The calculation of the axial phase velocity $v = w/\beta$ for $\epsilon_2(\rho) = \epsilon_1 [1 - d^2(\rho - r_2)^2 - d^4(\rho - r_2)^4]$ profile and for $r_1 = 0{\cdot}1$ cm, $r_2 = 0{\cdot}12$ cm and $d = 0{\cdot}38$ cm^{-1} shows that

(i) v_p decreases with increasing ϵ_3 and r_3/r_2;

(ii) v_p decreases with d.

8.4 *Guide Wavelength*

The calculation of the guide wavelength $\lambda_g = \omega/\beta$ for square-law and exponential profiles of which only the latter case is presented in Fig. 11, show that

(i) λ_g decreases and tends to attain a constant value of about $1{\cdot}5$ cm as ϵ_3 and r_3/r_2 increase;

(ii) λ_g decreases slightly with d.

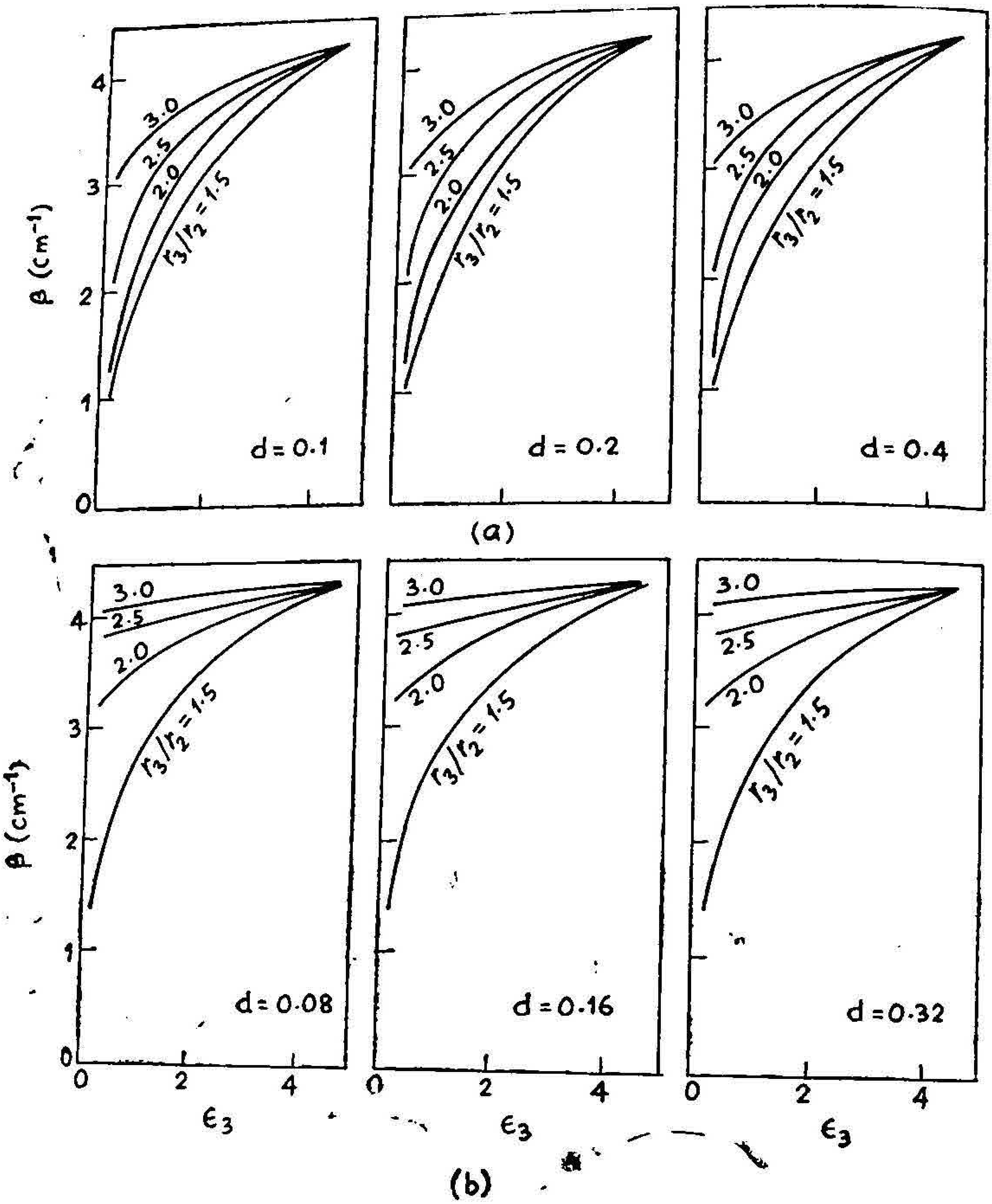

FIG. 10. Variation of β with ϵ_3

Profile : $\frac{\epsilon_3(\rho)}{\epsilon_1} = \operatorname{sech} d(\rho - r_3)$

(*a*) $r_1 = 0{\cdot}1$ cm, $r_2 = 0{\cdot}15$ cm.

(*b*) $r_1 = 0{\cdot}2$ cm, $r_2 = 0{\cdot}3$ cm.

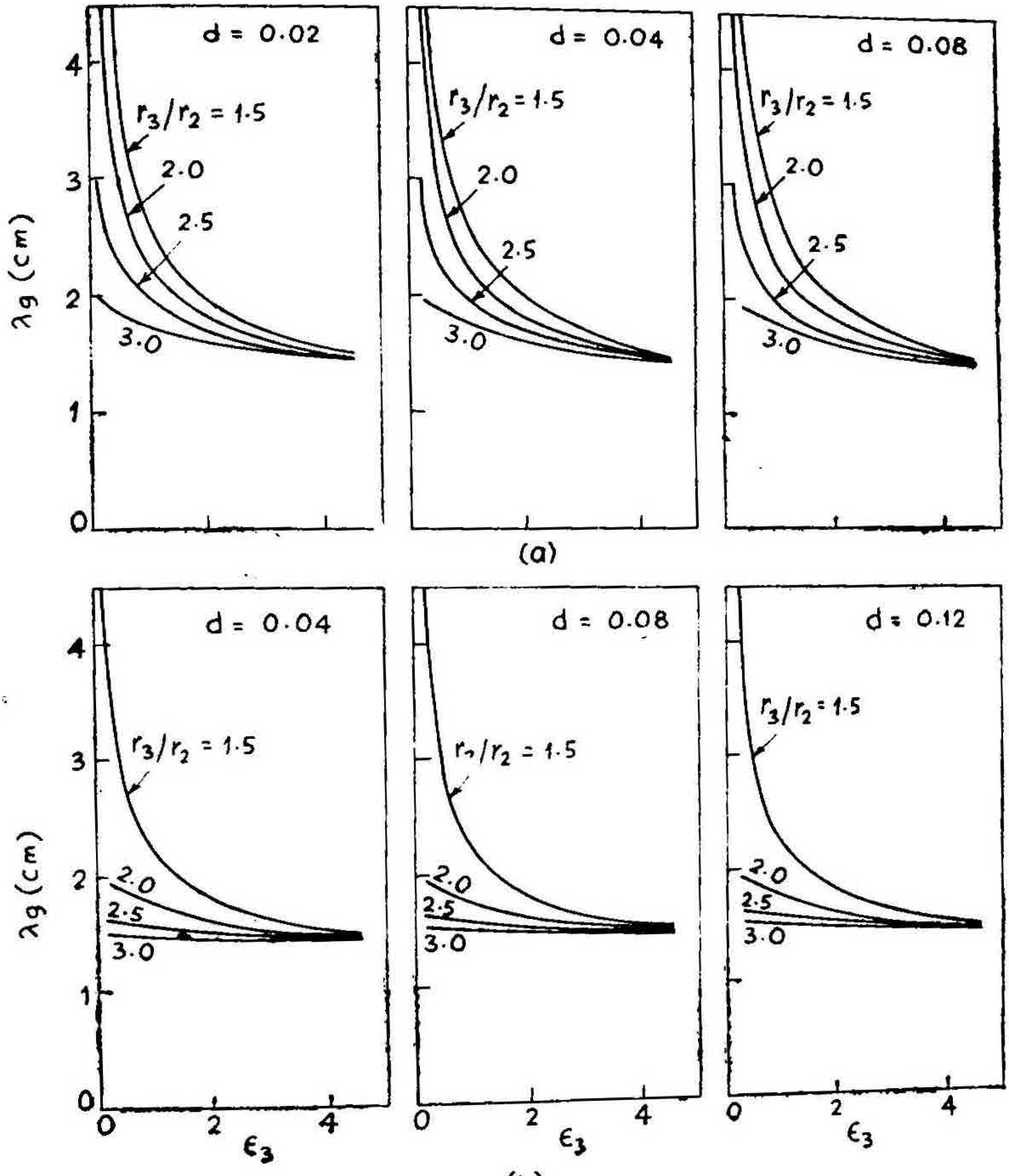

FIG. 11. Variation of λ_g with ϵ_3

Profile : $\frac{\epsilon_2(\rho)}{\epsilon_1} = \exp[-d(\rho - r_2)]$

$\lambda_0 = 3 \cdot 2$ cms

(*a*) $r_1 = 0 \cdot 1$ cm, $r_2 = 0 \cdot 15$ cm.

(*b*) $r_1 = 0 \cdot 2$ cm, $r_2 = 0 \cdot 3$ cm.

8.5 *Surface Reactions*

The surface reactance of the structure given by

$$X_s = \frac{a_3}{w\epsilon_0\epsilon_3} \cdot \frac{K_0(a_3r_3)}{K_1(a_3r_3)} \tag{13}$$

has been calculated for the square law and the fourth-power-law profiles for $r_1 = 0.1$ cm, $r_2 = 0,\ 12$ cm and r_3 0.62 cm. It is found that

(i) X_s decreases rapidly with ϵ^4 and is affected very little due to change in d.

(ii) The surface reactance in the case of the fourth-power-law is slightly higher than in the case of square-law profile.

9. POWER FLOW

The power flow in different media is calculated by using the Poynting vector and appropriate field components.

In medium 1 having dielectric constant ϵ_1, the power flow in the axial direction is,

$$P_{z1} = A_1A_1^* \frac{\pi\omega\epsilon_0\epsilon_1\beta}{2a_1^2Y_0^2(a_1r_1)}\Big\{(\rho^2[F_{00}^2(a_1\rho) + F_{10}^2(a_1\rho) - \frac{2}{a_1\rho}F_{00}(a_1\rho)F_{10}(a_1\rho)]\Big\}_{\rho=r_1}^{\rho=r_2} \tag{14}$$

where

$F_{00}(a_1\rho)$ and $F_{10}(a_1\rho)$ are given by equation (11 *b*).

The power flow in medium 2 is

$$P_{z2} = \frac{1}{2} Re \int_{\phi=0}^{2\pi} \int_{\rho=r_2}^{r_3} E_{\rho 2} H_{\phi 2}^* \rho d\rho\, d\phi$$

$$= \pi\omega\epsilon_0\beta C_1C_1^* \int_{\rho=r_2}^{r_3} \frac{\epsilon_2(\rho)}{a_2^4(\rho)} G_1^2(\rho)\, \rho d\rho \tag{15}$$

where

$$G_1(\rho) = S_3(\rho) + C' S_4(\rho)\ C' = C_2/C_1 \tag{15 a}$$

which is derived by using boundary conditions and appropriate field components and is given by

$$C' = \frac{C_2}{C_1} = -\left[\frac{\epsilon_2 F_{10}(a, r_2)\, S_1(r_2) + X(r_2)\, a_1\, F_{00}(a_1 r_2)\, S_3(r_2)}{\epsilon_1 F_{10}(a_1 r_2)\, S_2(r_2) + X(r_2)\, a_1 F_{00}(a_1 r_2)\, S_0(r_2)}\right] \quad (16)$$

Similarly,

$$C_1 C_1^* = \left[\frac{F_{00}(a_1 r_2)}{G_0(r_2)\, Y_0(a_1 r_2}\right]^2 A_1 A_1^* \quad (17)$$

where

$$G_0(\rho) = S_1(\rho) + C'' S_2(\rho).$$

Hence

$$P_{z2} = A_1 A_1^* \pi \omega \epsilon_0 \beta \left[\frac{F_{00}(a_1 r_2)}{G_0(r_2)\, Y_0(a_1 r_2)}\right]^2 \int_{\rho=r_2}^{r_3} \frac{\epsilon_2(\rho)\, G_1^2(\rho)}{a_2^4(\rho)}\, \rho\, d\rho. \quad (18)$$

The power flow in medium 3 is

$$P_{z3} = \frac{1}{2} Re \int_{\phi=0}^{2\pi} \int_{\rho=r_3}^{\infty} E_{\rho 3}\, H^*_{\phi 3}\, \rho\, d\rho\, d\phi$$

which yields

$$P_{z3} = \frac{2\omega \epsilon_0 \beta \epsilon_3}{\pi a_3^2} DD^* r_3^2 \Big[K_0^2(a_3 r_3) - K_1^2(a_3 r_3) + \frac{2}{a_3 r_3} K_0(a_3 r_3)\, K_1(a_3 r_3)\Big] \quad (19)$$

where

$$DD^* = \left(\frac{\pi}{2}\right)^2 \left[\frac{G_0(r_3)\, F_{00}(a_1 r_2)}{K_0(a_3 r_3)\, G_0(r_2)\, Y_0(a_1 r_1)}\right] A_1 A_1^*. \quad (19\,a)$$

Hence

$$P_{z3} = \frac{\pi \omega \epsilon_0 \epsilon_3 \beta}{2a_3^2} \left[\frac{G_0(r_3)}{G_0(r_2)} \; \frac{F_{00}(a_1 r_2)}{Y_0(a_1 r_2)\, K_0(a_3 r_3)}\right]^2 A_1 A_1^* F(a_3 r_3) \quad (20)$$

where

$$F(a_3 r_3) = r_3^2 \Big(K_0^2(a_3 r_3) - K_1^2(a_3 r_3) + \frac{2}{a_3 r_3} K_0(a r_3)\, K_1(a_3 r_3)\Big]. \quad (20\,a)$$

The percentages of power flow in different media with respect to the total axia power flow $P_{tot} = P_{z1} + P_{z2} + P_{z3}$ have been computed for different dielectric constant profiles as functions of ϵ_3 and r_3/r_2. Figure 12 shows the results for square law profile. It is observed that

(i) P_{z1} and P_{z2} increases but P_{z3} decreases with increase of ϵ_3

(ii) P_{z2} tends to attain a constant value as $\epsilon_3 \to \epsilon_1$.

10. POWER LOSS

The power loss is calculated by taking into account ohmic loss of the conductor and dielectric losses in respective media.

The power lost in the conductor is

$$P_{lc} = R_{sc}\,\pi\left(\frac{2\omega\epsilon_0\epsilon_1}{\pi a_1^2 r_1}\right) A_1 A_1^* \tag{21}$$

which is obtained by using the relation

$$P_{lc} = Re\left\{\frac{R_{sc}}{2}\int_0^{2\pi} [H_{\phi 1}\, H_{1\phi}^*]\right\}_{\rho = r_1} r_1 d\phi \tag{22}$$

where R_{sc}, the surface reactance of the conductor is given by the relation

$$R_{sc} = \left(\frac{\omega\mu_0}{2}\right)^{\frac{1}{2}} \tag{22 a}$$

The power lost in the dielectric medium having dielectric constant ϵ_1 and loss tangent tan δ is

$$P_{l1} = \tfrac{1}{2}\int_{\phi=0}^{2\pi}\int_{\rho=r_1}^{2\pi} \sigma_1\, |E_1|^2 \rho\, d\rho\, d\phi \tag{23}$$

where

$$\sigma_1 = \epsilon_0\epsilon_1 \tan\delta_1$$

and

$$|E_1|^2 = |E_{z1}|^2 + |E\rho_1|^2. \tag{23 a}$$

The equation (23) is evaluated to yield

$$P_{l1} = \pi\omega\epsilon_0\epsilon_1 \tan\delta_1\, A_1 A_1^* (1 + \beta^2/a_1^2) \times$$

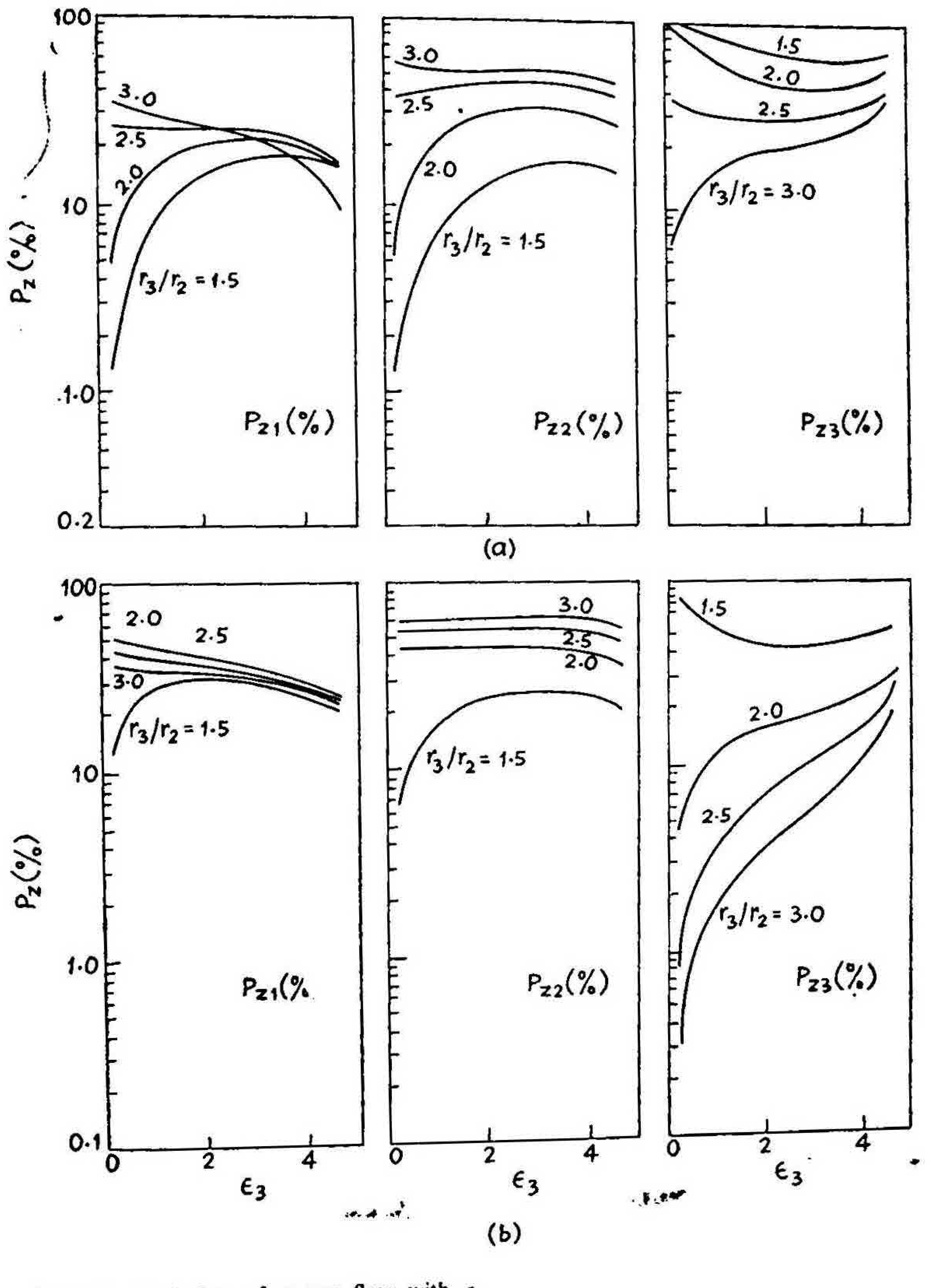

FIG. 12. Variation of power flow with ϵ_3

Profile : $\frac{\epsilon_2(\rho)}{\epsilon_1} = 1 - d^2(\rho - r_2)^2$

(*a*) $r_1 = 0 \cdot 1$ cm, $r_2 = 0 \cdot 15$ cm.

(*b*) $r_1 = 0 \cdot 2$ cm, $r_2 = 0 \cdot 3$ cm.

$$\times \left[\frac{\rho^2}{2} \left\{F_{00}^2(a_1\rho) + F_{10}^2(a_1\rho) - \frac{2}{a_1\rho}\left(\frac{\beta^2}{a_1^2+\beta^2}\right) \times F_{00}(a_1\rho)\, F_{10}(a_1\rho)\right\}\right]_{\rho=r_1}^{\rho=r_2} \tag{24}$$

Similarly, the power lost in medium 2 is given by

$$P_{l2} = \pi\omega\epsilon_0 \tan\delta_2\, C_1 C_1^* \int_{\rho=r_2}^{r_3} \epsilon_2(\rho)\left[G_0^2(\rho) + \frac{\beta^2}{a_2^4(\rho)} G_1^2(\rho)\right]\rho\, d\rho \tag{25}$$

and the power lost in the external medium is

$$P_{l3} = \frac{2\omega\epsilon_0\epsilon_3 \tan\delta_3}{\pi} DD^* r_3^2\left(\frac{\beta^2 - a_3^2}{a_3^2}\right)\left[K_0^2(a_3r_3) - K_1^2(a_3r_3) + \frac{2}{a_3r_3}\left(\frac{\beta^2}{\beta^2 - a_3^2}\right)K_0(a_3r_3)\, K_1(a_3r_3)\right] \tag{26}$$

11. ATTENUATION CONSTANT

The attenuation constant of the surface wave line is obtained by using the relation

$$\alpha = \frac{P_l}{2\, P_{tot}} \tag{27}$$

where

$$P_l = P_{lc} + P_{l1} + P_{l2} + {}_lP_{3}$$

P_{tot} = total power flow.

The attenuation constant has been calculated for lines having different profiles. Figure 13 shows the variation of α with respect to ϵ_3 for different values of $\tan\delta$ and for square law profile. It is observed that α increases and then gradually decreases for small values of r_3 and it decreases for large values of r_3 as ϵ_3 increases.

12. CHARACTERISTIC EQUATION FOR A CONDUCTOR COATED WITH TWO HOMOGENEOUS DIELECTRICS

In order to compare the surface wave characteristics of the above cases with the characteristics of a conductor coated with two homogeneous dielectrics the characteristic equation has been formed as follows.

$$\left[\frac{\epsilon_3}{a_3} K_1(a_3r_3)\, Y_0(a_2r_3) + \frac{\epsilon_2}{a_2} K_0(a_3r_3)\, Y_1(a_2r_3)\right]$$

$$\times \left[\frac{\epsilon_1}{a_1} J_0(a_2r_2)\, F_{10}(a_1r_2) - \frac{\epsilon_2}{a_2} J_1(a_2r_2)\, F_{00}(a_1r_2)\right]$$

$$- \left[\frac{\epsilon_3}{a_3} K_1(a_3r_3)\, J_0(a_2r_3) + \frac{\epsilon_2}{a_2} K_0(a_3r_3)\, J_1(a_2r_3)\right]$$

$$\times \left[\frac{\epsilon_1}{a_1} Y_0(a_2r_2)\, F_{10}(a_1r_2) - \frac{\epsilon_2}{a_2} Y_1(a_2r_2)\, F_{00}(a_1r_2)\right] = 0 \qquad (28)$$

by using proper boundary conditions at the interface between media 1 and 2 and appropriate field components. The field components in medium 2 are

$$E_{z2} = [C_1 J_0(a_2\rho) + C_2 Y_0(a_2\rho)]\, e^{j(wt-\beta z)}$$

$$E_{\rho 2} = \frac{j\beta}{a_2} [C_1 J_1(a_2\rho) + C_2 Y_1(a_2\rho)]\, e^{j(wt-\beta z)}$$

$$H_{\phi 2} = \frac{j\omega \epsilon_0 \epsilon_2}{a_2} [C_1 J_1(a_2\rho) + C_2 Y_1(a_2\rho)]\, e^{j(wt-\beta z)} \qquad (29)$$

which are obtained by solving

$$\nabla^2 E + k_0^2 \epsilon_2 E = 0$$

and utilising Maxwell's equation.

The characteristic equation has been solved by using the relations

$$a_1^2 = a_3^2 = k_0^2(\epsilon_1 - \epsilon_3)$$

$$a_2^2 + a_3^2 = k_0^2(\epsilon_2 - \epsilon_3) \qquad (30)$$

to yield values of the radial propagation constants a_1, a_2, a_3 and also β, λ_g and v_p (Figs. 14 to 16), which show that

(i) a_1 decreases with ϵ_2 and ϵ_3

(ii) a_2 and a_3 decrease with ϵ_3 but increase with ϵ_2

(iii) β increases with ϵ_2 and ϵ_3

(iv) λ_g and v_p decrease with increasing ϵ_2 and ϵ_3

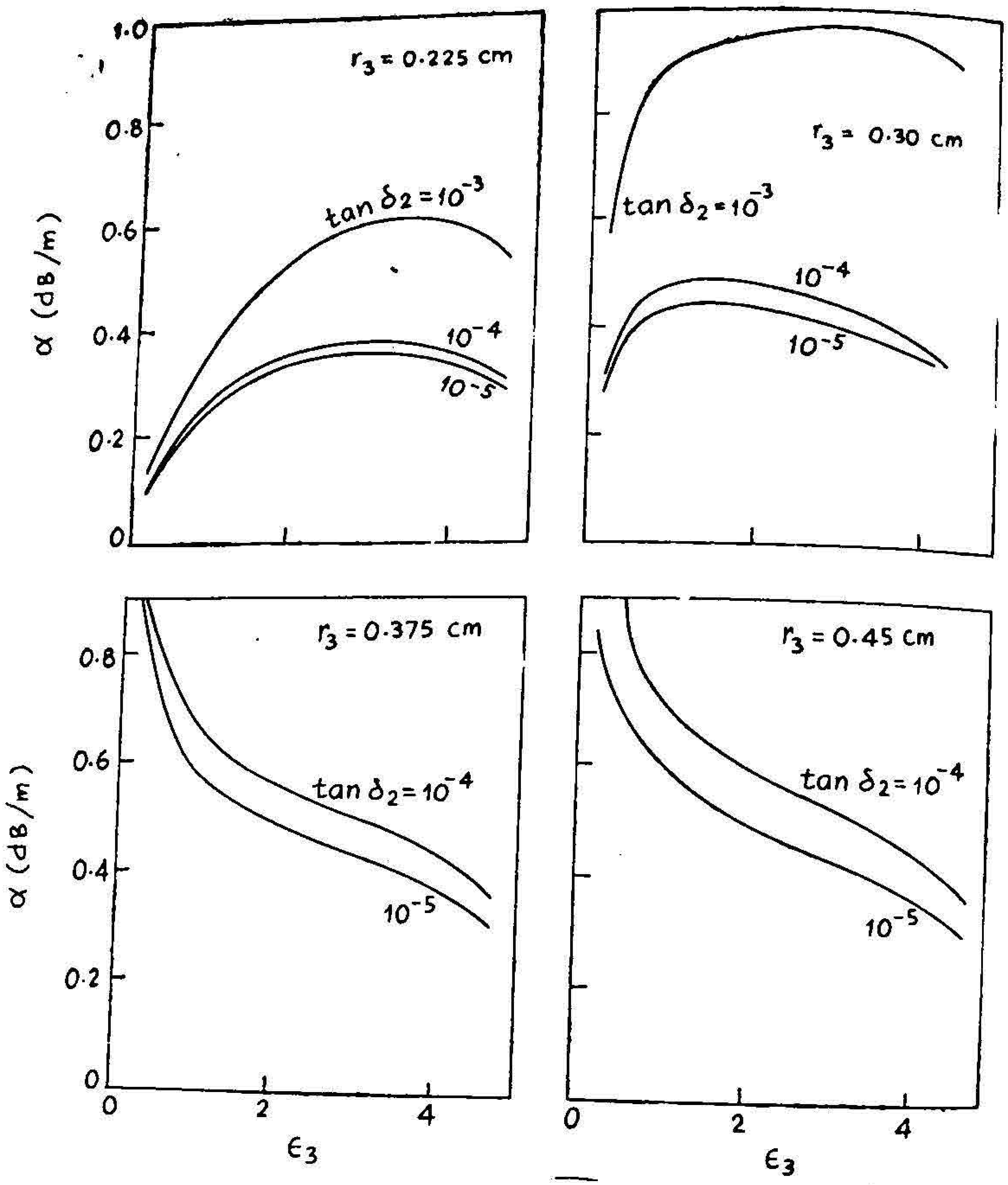

FIG. 13. Variation of α with ϵ_3

Profile : $\frac{\epsilon_2(\rho)}{\epsilon_1} = 1 - d^2(\rho - r_2)^2$

(a) $r_1 = 0\cdot1$ cm, $r_2 = 0\cdot15$ cm.

(b) $r_1 = 0\cdot2$ cm, $r_2 = 0\cdot3$ cm.

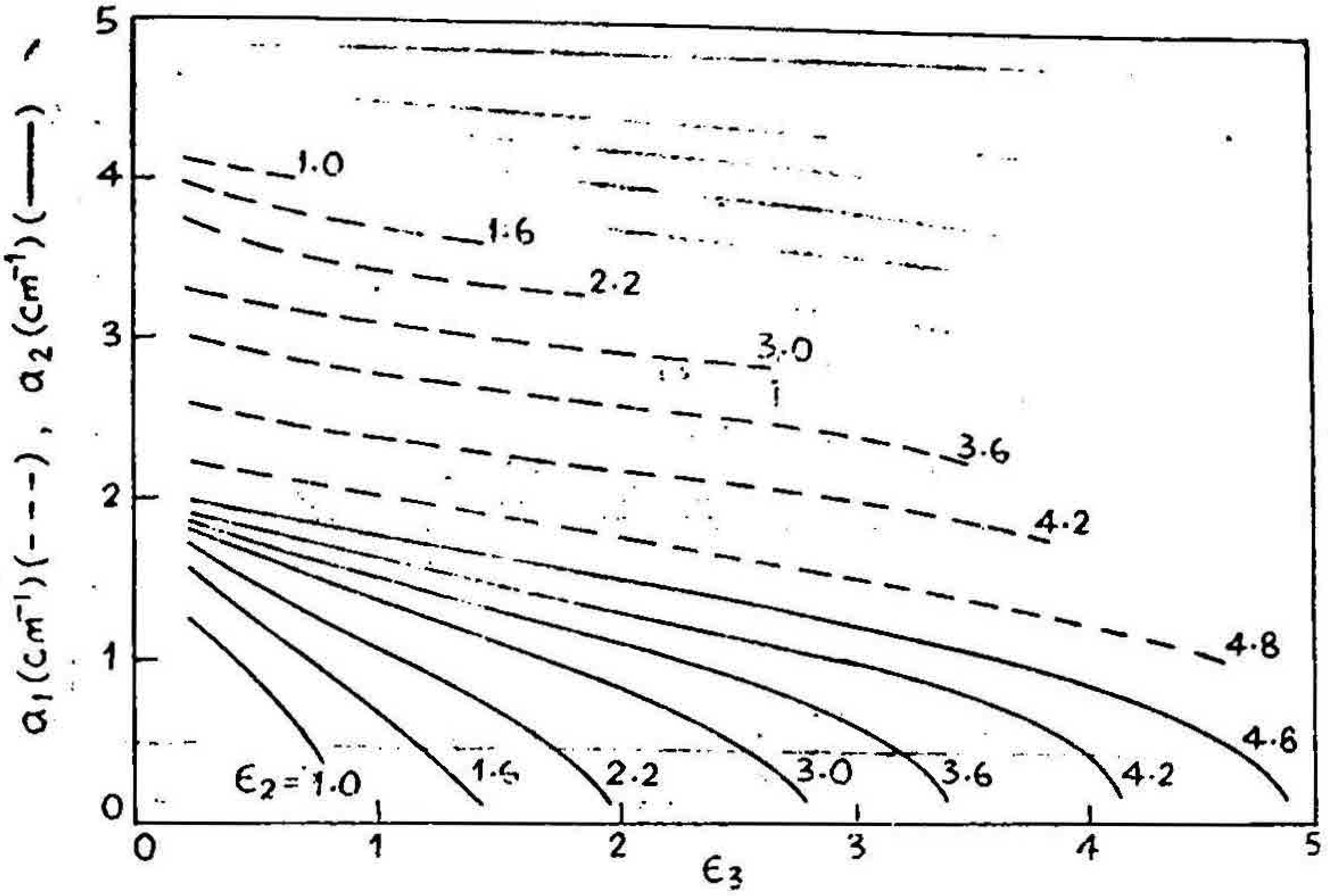

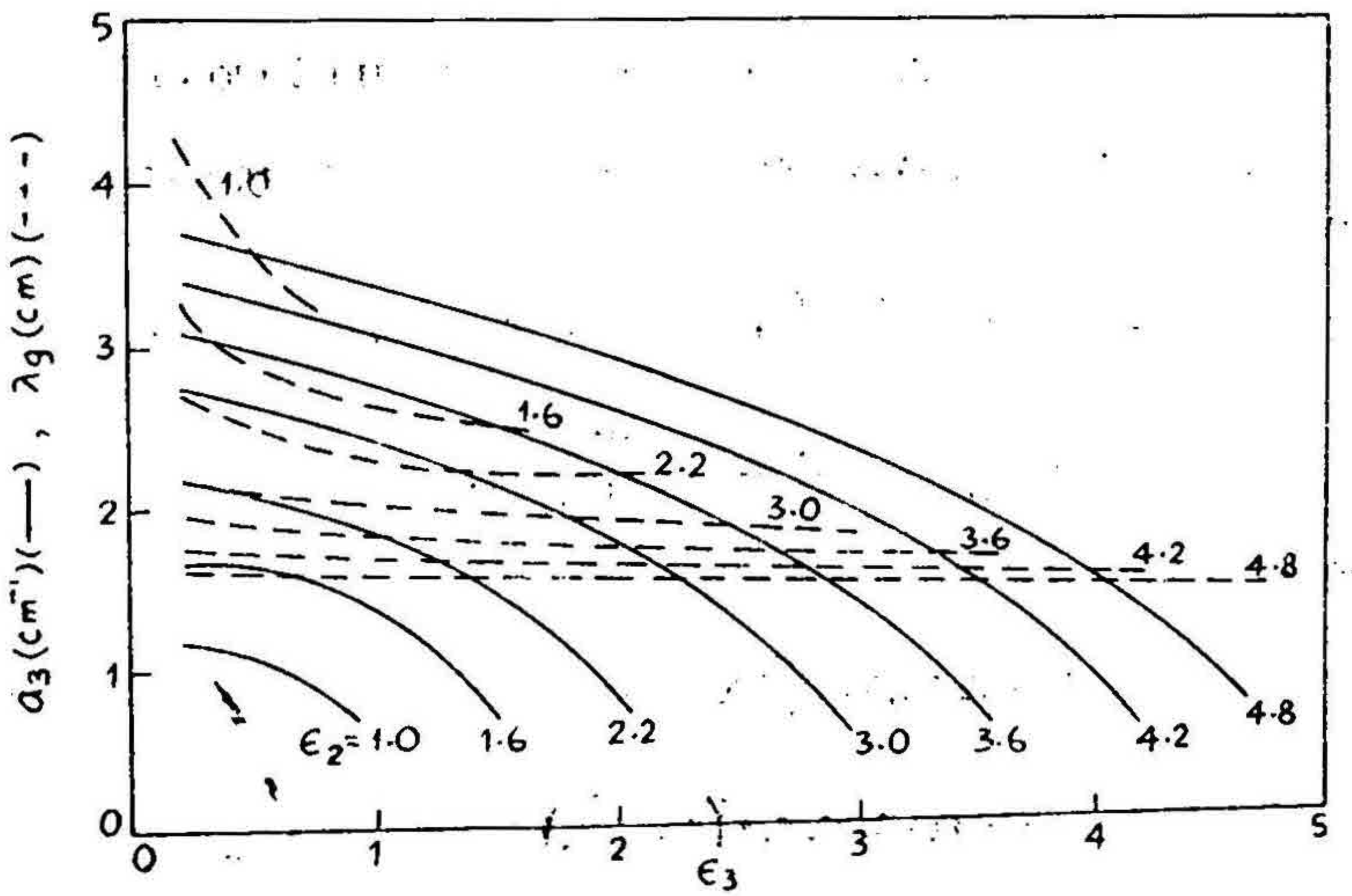

FIG. 14. Plots of a_1 and a_2 for a homogeneous case
$r_1 = 0.1$ cm, $r_2 = 0.12$ cm, $r_3 = 0.62$ cm, $\epsilon_1 = 5.0$.

FIG. 15. Plots of a_3 and λ_g for a homogeneous case
$r_1 = 0.1$ cm, $r_2 = 0.12$ cm, $r_3 = 0.62$ cm, $\epsilon_1 = 5.0$.

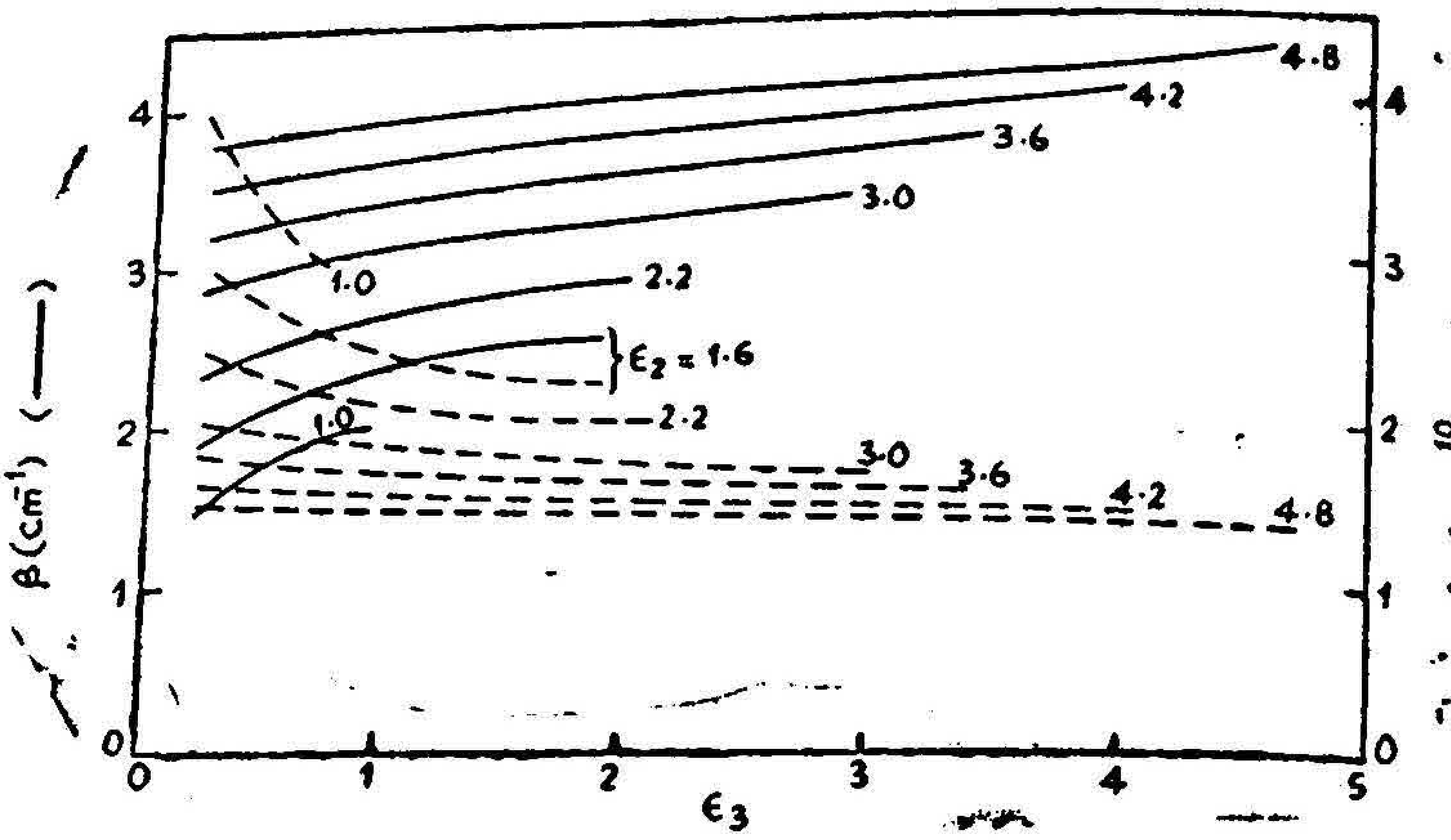

FIG. 16. Plots of β and v_p for a homogeneous case $r_1 = 0\cdot 1$ cm, $r_2 = 0\cdot 12$ cm, $r_3 = 0\cdot 62$ cm, $\epsilon_1 = 5\cdot 0$.

13. Power Flow and Attenuation Constant of the Homogeneous Line

The power flow P_{z2} and power lost P_{l2} in the second medium are given respectively

$$P_{z2} = C_1 C_1{}^* \frac{2\pi\omega\epsilon_0\epsilon_2\beta}{a_2{}^2}\Big[G_{00}{}^2(a_2\rho) + G_{10}{}^2(a_2\rho) - \frac{2}{a_2\rho} G_{00}(a_2\rho)\, G_{10}(a_2\rho)\Big]_{\rho=r_2}^{r_3} \tag{31}$$

where

$$G_{r0}(a_2\rho) = J_r(a_2\rho) + \frac{C_2}{C_1} Y_r(a_2\rho) \tag{31 a}$$

$$P_{l2} = \pi\omega\epsilon_0\epsilon_2 \tan\delta_2\, C_1 C_1{}^*\Big(1 + \frac{\beta^2}{a_2{}^2}\Big) \times \Big[\frac{\rho^2}{2}\Big\{G_{00}{}^2(a_2\rho) + G_{10}{}^2(a_2\rho) - \frac{2}{a_2\rho}\Big(\frac{\beta^2}{a_2{}^2 + \beta^2}\Big) \times G_{00}{}^2(a_2\rho)\, G_{10}(a_2\rho)\Big\}\Big]_{\rho=r_2}^{r_3}. \tag{32}$$

Using the expressions (14, 20) for power flow and (24, 26) for power loss in media 1 and 3, division of power in different media and attenuation constant are evaluated. The results are shown in Fig. 17. The dielectric constant of the second dielectric coating is $\epsilon_1 (1 - 0{\cdot}04)$ which is comparable to the gradually varying inhomogeneous dielectric profiles.

It is found that of all the six different cases, the fourth power profile, shows the best behaviour as far as the concentration of power flow is concerned, but the attenuation constant is more in this case than the other cases.

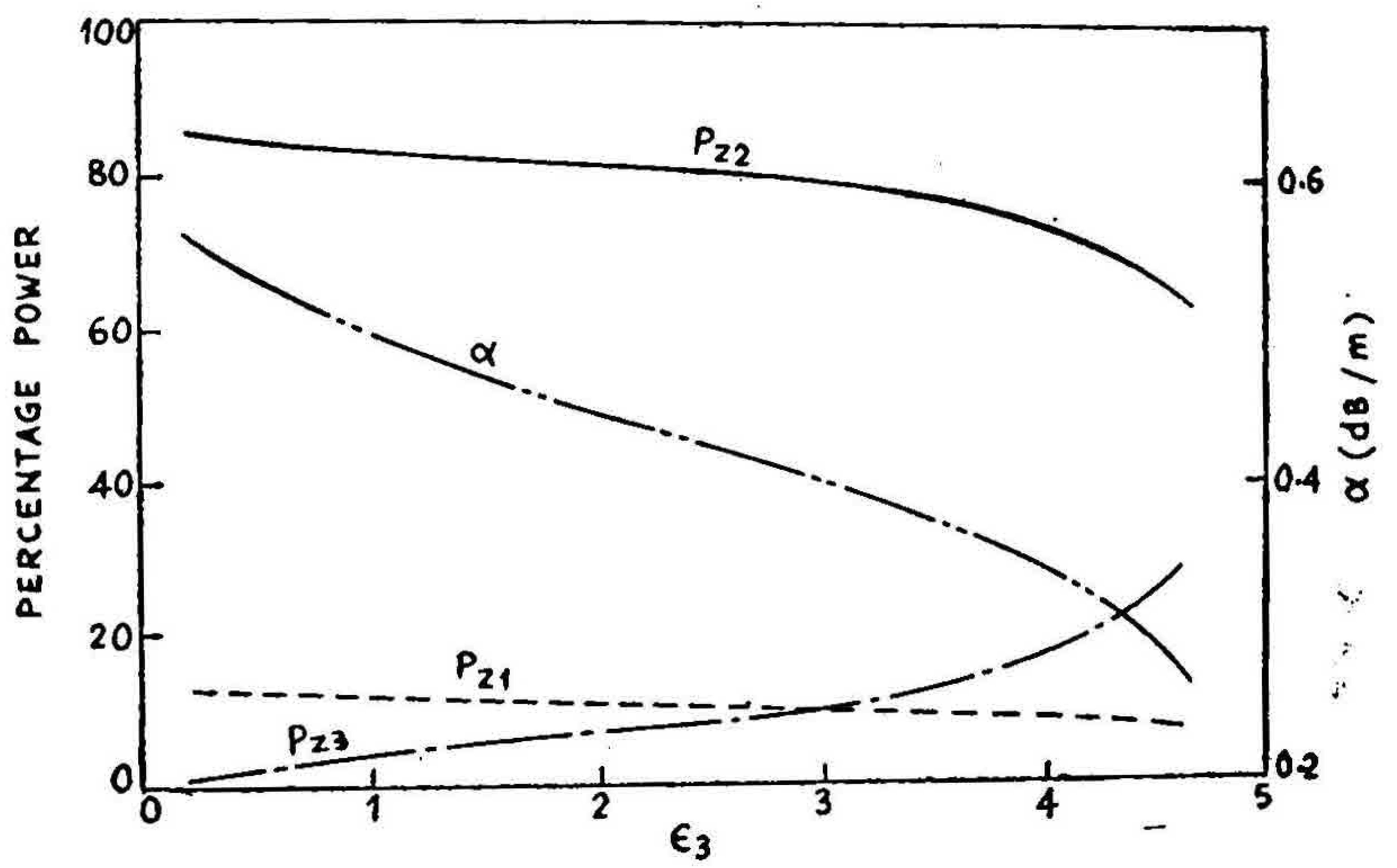

FIG. 17. Plots of P_z and α for a homogeneous case
$r_1 = 0{\cdot}1$ cm, $r_2 = 0{\cdot}12$ cm, $r_3 = 0{\cdot}62$ cm, $\epsilon_1 = 5{\cdot}0$, $\epsilon_2 = 4{\cdot}8$.

14. Conductor Coated with Two Graded Dielectrics

The two profiles that have been considered are the

(i) Quadratic profile, and

(ii) fourth-power profile.

The dielectric profiles in both the media are (Fig. 1)

Case (i) quadratic profile

Med. 1 $(r_1 \leq \rho \leq r_2)$

$$\epsilon_1 (\rho) = \epsilon_1 [1 + d^2 (\rho - r_1)^2]/[1 + d^2 (r_2 - r_1)^2]$$

Med. 2 $(r_2 \leq \rho \leq r^4)$

$$\epsilon_2(\rho) = \epsilon_1 [1 - d^2 (\rho - r_2)^2]. \quad (33)$$

Case (ii) fourth-power profile

Med. 1 $(r_1 \leq \rho \leq r_2)$

$$\epsilon_1(\rho) = \epsilon_1 [1 + d^4 (\rho - r_1)^4]/[1 + d^4 (r_2 - r_1)^4].$$

Med. 2 $(r_2 \leq \rho \leq r_3)$

$$\epsilon_2(\rho) = \epsilon_1 [1 - d^4 (\rho - r_2)^4]. \quad (34)$$

Hence for $\rho = r_1$

Case (i) $\epsilon_1(\rho) = \epsilon_1/[1 + d^2 (r_2 - r_1)^2]$

Case (ii) $\epsilon_1(\rho) = \epsilon_1/[1 + d^4 (r_2 - r_1)^4]$

For $\rho = r_2$

Case (i) $\epsilon_1(\rho) = \epsilon_2(\rho) = \epsilon_1$

Case (ii) $\epsilon_1(\rho) = \epsilon_2(\rho) = \epsilon_1$ (35)

The wave equation in medium 1 is

$$\nabla^2 E + k_0^2 \epsilon_1(\rho) E = 0$$

which yields the following field components

$$E_{z1} = [A_1 R_1(\rho) + A_2 R_2(\rho)]\, e^{j(\omega t - \beta z)}$$

$$E_{\rho 1} = \frac{-j\beta}{a_1^2(\rho)} [A_1 R_3(\rho) + A_2 R_4(\rho)]\, e^{j(\omega t - \beta z)}$$

$$H_{\phi 1} = \frac{-j\omega \epsilon_0 \epsilon_1(\rho)}{a_1^2(\rho)} [A_1 R_3(\rho) + A_2 R_4(\rho)]\, e^{j(\omega t - \beta z)} \quad (36)$$

The functions $R_1(\rho)$ and $R_2(\rho)$ are the two independent solutions of the wave equation and $R_3(\rho)$ and $R_4(\rho)$ are the derivatives of $R_1(\rho)$ and $R_2(\rho)$ respectively, with respect to ρ.

The axial and radial propagation constants are related as

$$a_1^2(\rho) = k_0^2 \epsilon_1(\rho) - \beta^2$$

$$a_2^2(\rho) = k_0^2 \epsilon_2(\rho) - \beta^2$$

$$a_3^2 = \beta^2 - k_0^2 \epsilon_3. \quad (37)$$

By using proper boundary conditions and appropriate field components, the following characteristic equation is obtained

$$\left[\frac{\epsilon_3}{a_3} K_1(a_3r_3)\, S_2(r_3) - X(r_3)\, K_0(a_3r_3)\, S_0(r_3)\right]$$
$$\times\ [X(r_2)\, S_3(r_2)\, P_0(r_2) - Y(r_2)\, S_1(r_2)\, P_1(r_2)]$$
$$-\left[\frac{\epsilon_3}{a_3} K_1(a_3r_3)\, S_1(r_3)\, S_1(r_3) - X(r_3)\, K_0(a_3r_3)\, S_3(r_3)\right]$$
$$\times\ [X(r_2)\, S_4(r_2)\, P_0(r_2) - Y(r_2)\, S_2(r_2)\, P_1(r_2)] = 0 \tag{38}$$

where

$$P_0(\rho) = R_1(r_1)\, R_2(\rho) - R_1(\rho)\, R_2(r_1)$$
$$P_1(\rho) = R_1(r_1)\, R_4(\rho) - R_3(\rho)\, R_2(r_1)$$
$$X(\rho) = \epsilon_2(\rho)/a_2^2(\rho)$$
$$Y(\rho) = \epsilon_1(\rho)/a_1^2(\rho). \tag{38 a}$$

The characteristic equation has been solved with the aid of the following two equations:

$$a_1^2(\rho) + a_3^2 = k_0^2\epsilon_1(\rho) - \epsilon_3$$
$$a_2^2(\rho) + a_3^2 = k_0^2\,\epsilon_2(\rho) - \epsilon_3. \tag{38 b}$$

The solution of the characteristic equation yields $a_1(\rho)$, $a_2(\rho)$ and a_3 from which β, v_p and λ_g are derived.

The power flowing in medium 1 is given by

$$P_{z1} = \pi\omega\epsilon_0\beta A_1A_1^* \int_{\rho=r_1}^{r_2} \frac{\epsilon_1(\rho)}{a_1^4(\rho)} \frac{R_1^2(\rho)}{P_1^2(\rho)}\, \rho d\rho \tag{39}$$

where $P_1(\rho)$ is given by equation (38 *a*).,The power lost in the conductor is given by

$$P_{lc} = Re\left\{\frac{R_{sc}}{2} \int_0^{2\pi} [H_{\phi1}\, H_{\phi1}^*]_{\rho=r_1}\right\} r_1 d\phi$$

which yields

$$P_{lc} = A_1A_1^*\,\pi\left[\frac{\omega\epsilon_0\epsilon_1(r_1)}{a_1^2(r_1)} \frac{P_1(r_1)}{R_2(r_1)}\right]^2 \tag{40}$$

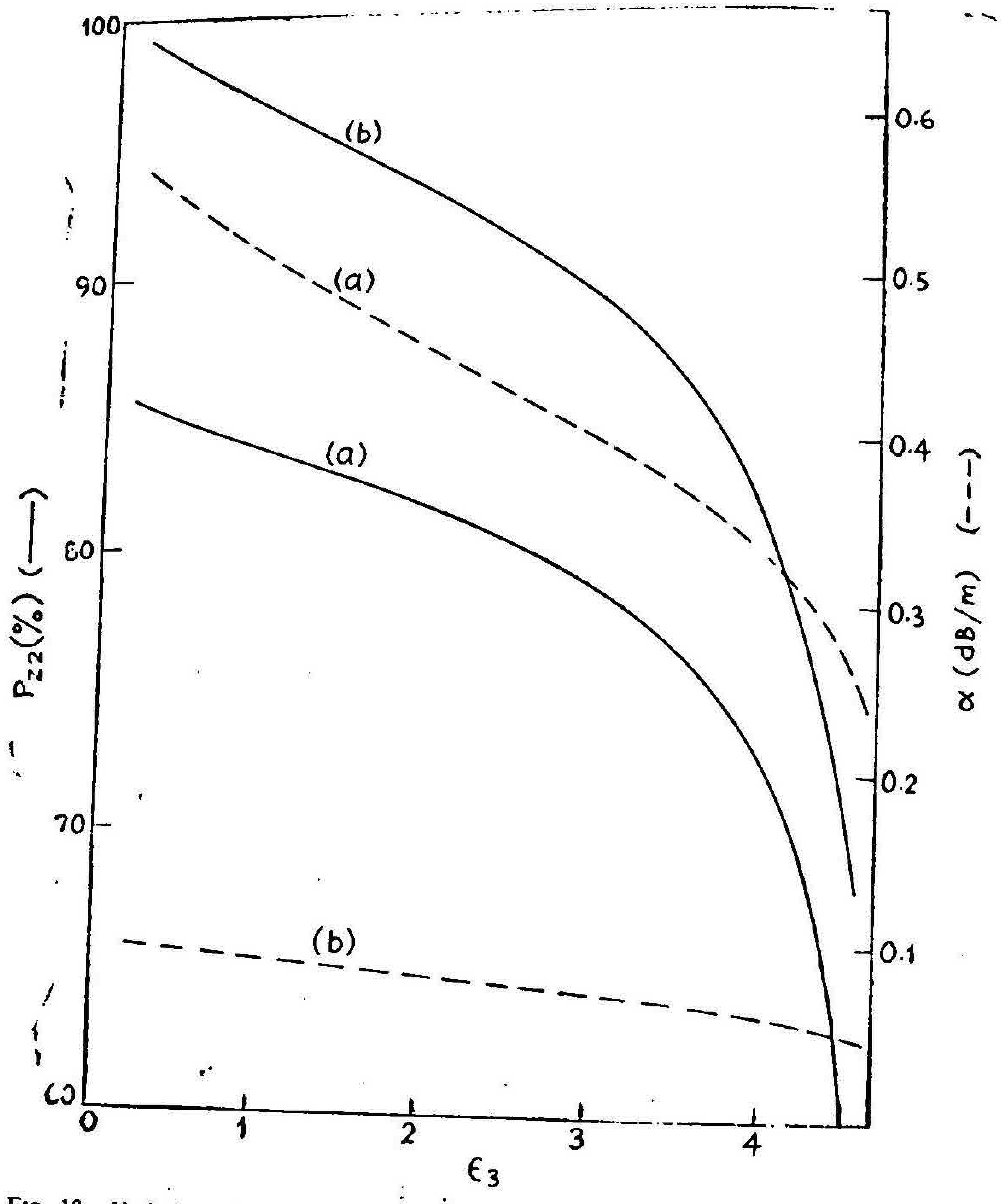

FIG. 18. Variation of P_{z2} and α with ϵ_3
(*a*) single-graded dielectric-coated line
(*b*) doubly-graded dielectric-coated line.

Power lost in medium 1 is

$$P_{l1} = \frac{\pi \omega \epsilon_0 \tan \delta_1}{R_2^2 (r_1)} A_1 A_1^* \int_{\rho = r_1}^{r_2} \epsilon (\rho) \left[P_0^2 (\rho) + \frac{\beta^2}{a_1^4 (\rho)} P_1^2 (\rho) \right] \rho d\rho. \quad (41)$$

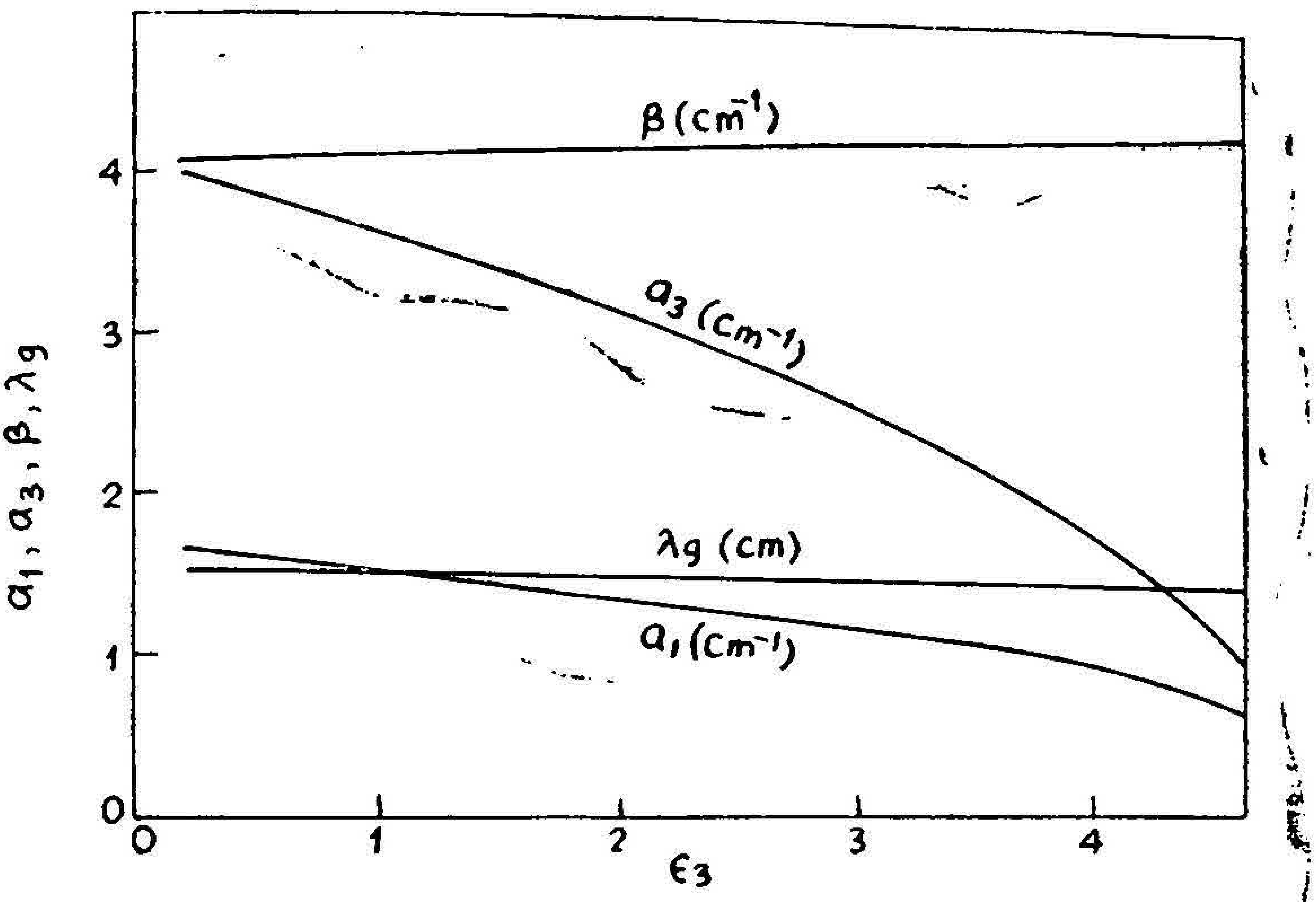

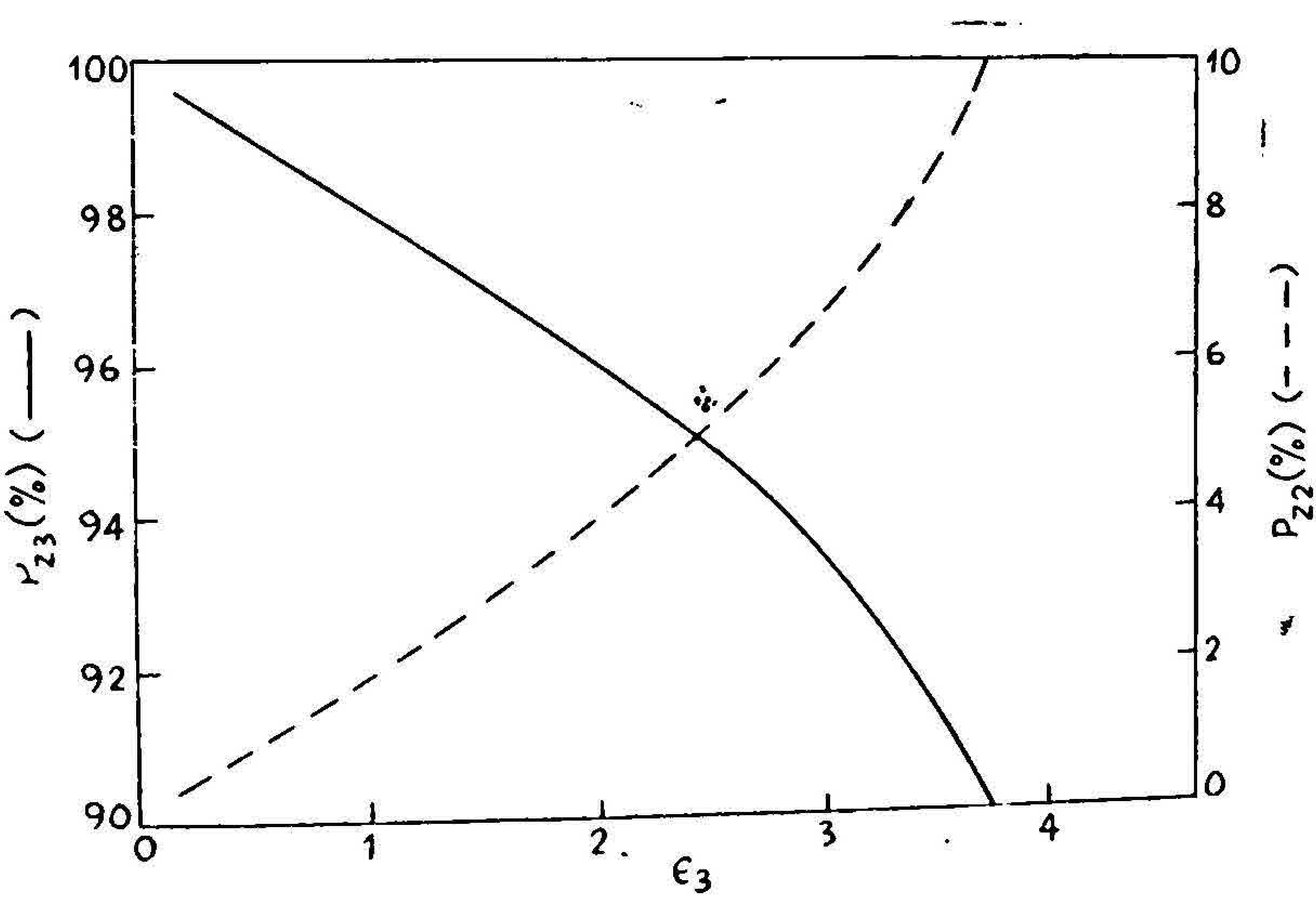

FIG. 19 *a*. Variation of a_1, a_3, λ_g and β with ϵ_3
$r_1 = 0\cdot1$ cm, $r_2 = 0\cdot12$ cm, $r_3 = 0\cdot62$ cm, $d = 0\cdot2$ cm^{-1}
Profile : Quadratic (doubly-graded).

FIG. 19 *b*. Variation of P_{22} and P_{23} with ϵ_3
$r_1 = 0\cdot1$ cm, $r_2 = 0\cdot12$ cm, $r_3 = 0\cdot62$ cm, $d = 0\cdot2\,cm^{-1}$
Profiles: Quadratic (doubly-graded).

The power flow and power lost in mdia 2 and 3 are given by equations (18) (20), (25) and (26) respectively. The division of power flow in different media and the attenuation constant are determined as in previous sections.

The results of numerical computations are presented in Figs. 18–22. In Fig. 22, α_c, α_{d1}, α_{d2} and α_{d3} represent the attenuations in conductor and the three dielectric media respectively.

The following conclusions can be drawn.

(1) In the case when both the dielectrics are graded, the power flow in medium 1 is less than in the case when one of the dielectric coatings is homogeneous and the outer dielectric is graded. This results in lower attenuation in the case when both the dielectrics are graded.

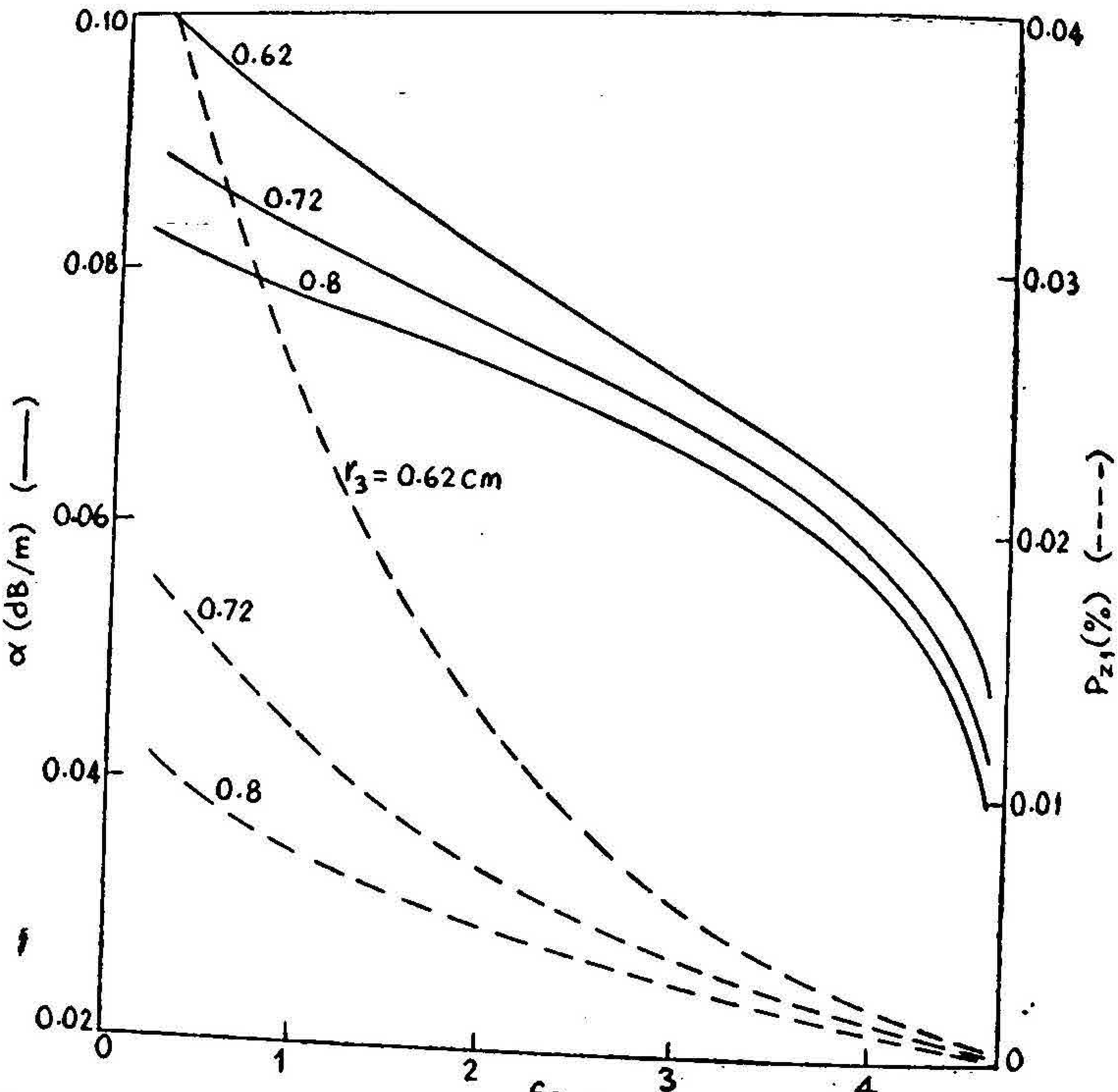

FIG. 20. Plots of α and P_{z1}
Profiles : Quadratic (doubly-graded)
$r_1 = 0.1$ cm, $r_2 = 0.12$ cm, $\epsilon_1 = 5.0$, $d = 0.2$ cm^{-1}.

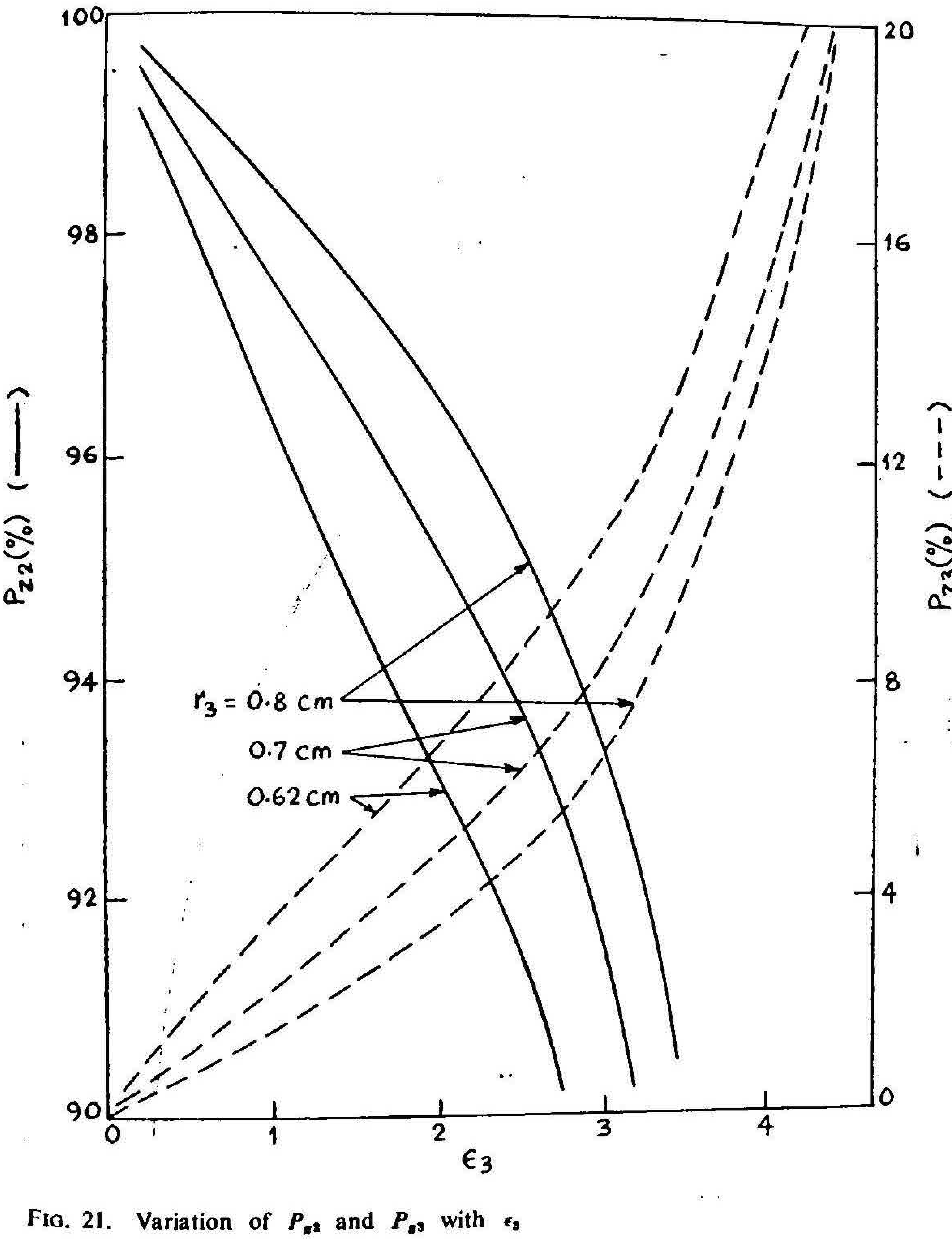

FIG. 21. Variation of P_{z2} and P_{z3} with ϵ_3

Profiles : Quadratic (doubly-graded)

$r_1 = 0 \cdot 1$ cm, $r_2 = 0 \cdot 12$ cm, $\epsilon_1 = 5 \cdot 0$, $d = 0 \cdot 2$ cm^{-1}.

(ii) α_c, α_{d1}, α_{d2} decrease with ϵ_3 while α_{d3} increases with ϵ_3.

(iii) As the thickness of the inhomogeneous medium increases, P_{z2} increases but α also increases.

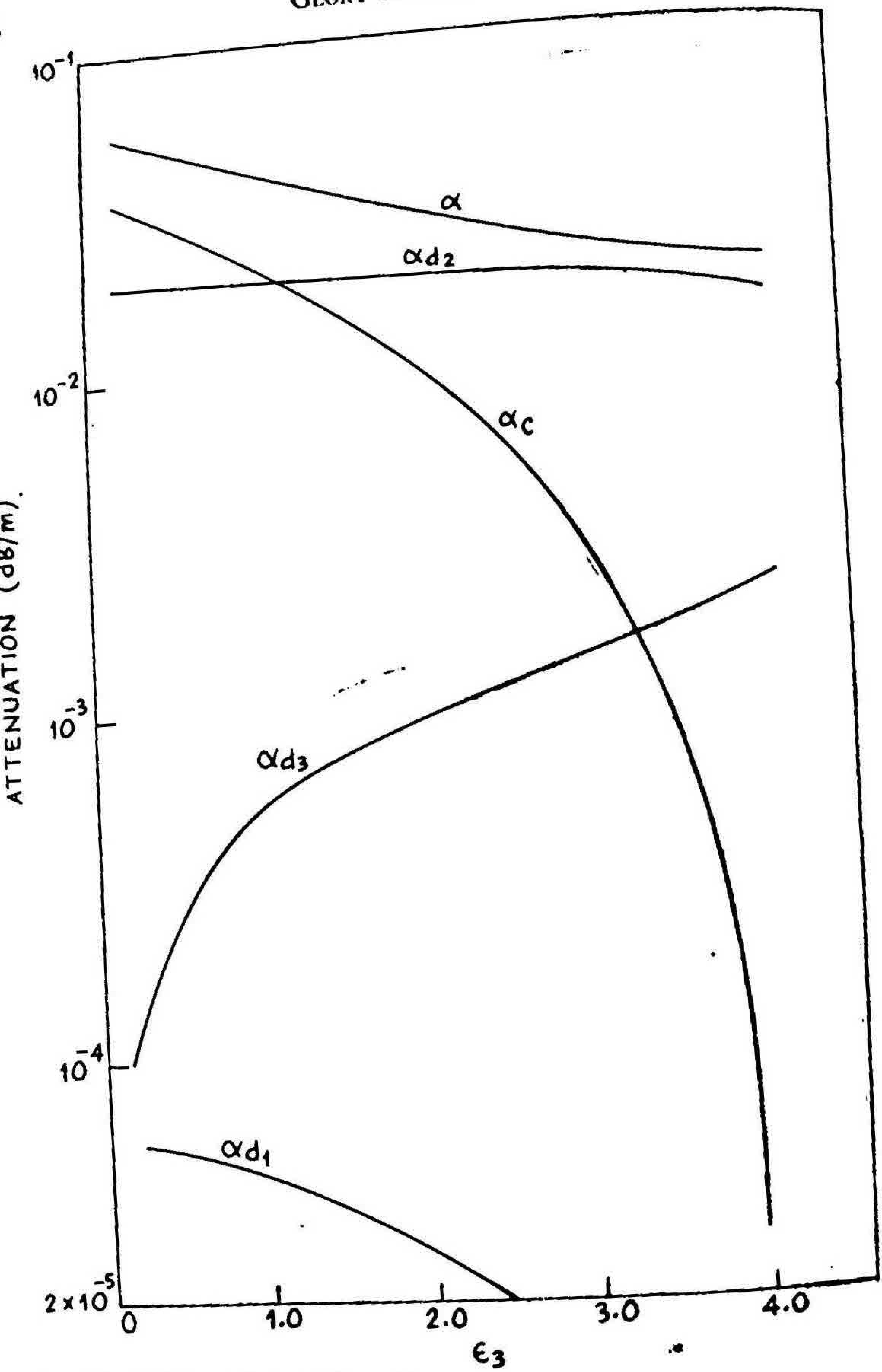

FIG. 22. Variation of attenuation with ϵ_3.

Profiles : Fourth power (doubly-graded)

$r_1 = 0 \cdot 1$ cm, $r_2 = 0 \cdot 12$ cm, $r_3 = 0 \cdot 72$ cm, $d = 0 \cdot 2\,\text{cm}^{-1}$

$\epsilon_1 = 5 \cdot 0$, $\tan \delta_1 = \tan \delta_2 = \tan \delta_3 = 0 \cdot 00001$, $= 5 \cdot 8 \times 10^5$ mhos/m

(iv) The radial propagation constants and other characteristics such as λ_g etc. do not vary significantly in the two cases when one of the dielectrics is homogeneous and when both the dielectric coatings are inhomogeneons.

15. Effect of Anisotropy

The wave equation in the external medium is

$$\frac{\partial^2 E_z}{\partial \rho^2} + \frac{1}{\rho}\frac{\partial E_z}{\partial \rho} + \left(\frac{\epsilon_z}{\epsilon_\rho}\right)\frac{\partial^2 E_z}{\partial z^2} + k_0^2\, \epsilon_z E_z = 0 \tag{42}$$

where

$$\epsilon_3 = \begin{pmatrix} \epsilon_\rho & 0 & 0 \\ 0 & \epsilon_\rho & 0 \\ 0 & 0 & \epsilon_z \end{pmatrix} \tag{43}$$

considering the $(\rho - \phi)$ plane as homogeneous and isotropic and hence taking $\epsilon_\phi = \epsilon_\rho$.

The field components in the external medium obtain by solving equation (42) and applying approriate Maxwell's equations are

$$E_{z3} = D H_0^{(1)}(ja_3\rho) e^{j(wt-\beta z)}$$

$$E_{\rho 3} = D\frac{\beta}{a_3}\left(\frac{\epsilon_z}{\epsilon_\rho}\right) H_1^{(1)}(ja_3\rho)\, e^{j(wt-\beta z)}$$

$$H_{\phi 3} = D\frac{k_0^2\, \epsilon_\rho}{\omega\mu_0 a_3}\left(\frac{\epsilon_z}{\epsilon_\rho}\right) H_1^{(1)}(ja_3\rho)\, e^{j(wt-\beta z)} \tag{44}$$

The radial and axial propagation constants in medium 3 are related by

$$a_3^2 = \frac{\epsilon_z}{\epsilon_\rho}(\beta^2 - k_3^2) \tag{45}$$

The characteristic equations for the three different cases are, (i) Conductor with two homogeneous dielectrics,

$$\begin{aligned}
&\left[\frac{\epsilon_z}{a_3} K_1(a_3r_3)\, Y_0(a_2r_3) + \frac{\epsilon_2}{a_2} K_0(a_3r_3)\, Y_1(a_2r_3)\right] \\
&\qquad \times \left[\frac{\epsilon_1}{a_1} J_0(a_2r_2)\, F_{10}(a_1r_2) - \frac{\epsilon_2}{a_2} J_1(a_2r_2)\, F_{00}(a_1r_2)\right] \\
&- \left[\frac{\epsilon_z}{a_3} K_1(a_3r_3)\, J_0(a_2r_3) + \frac{\epsilon_2}{a_2} K_0(a_3r_3)\, J_1(a_2r_3)\right] \\
&\qquad \times \left[\frac{\epsilon_1}{a_1} Y_0(a_2r_2)\, F_{10}(a_1r_2) - \frac{\epsilon_2}{a_2} Y_1(a_2r_2)\, F_{00}(a_1r_2)\right] = 0
\end{aligned} \tag{46}$$

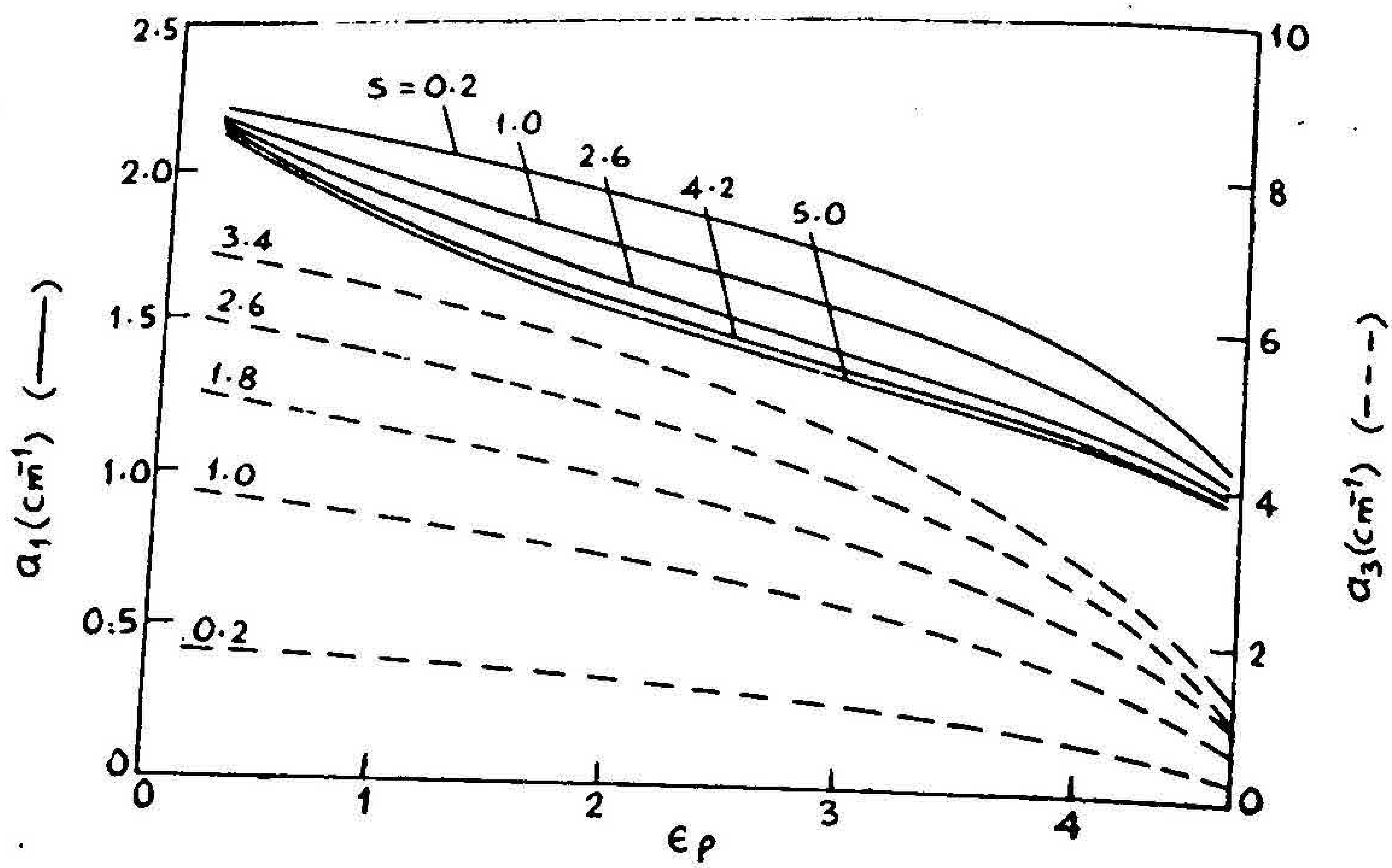

FIG. 23. Variation of a_1 and a_3 with ϵ_p
$r_1 = 0 \cdot 1$ cm, $r_2 = 0 \cdot 12$ cm, $r_3 = 0 \cdot 62$ cm, $\epsilon_1 = 5 \cdot 0$, $\epsilon_3 = 4 \cdot 8$, $s = \epsilon_s/\epsilon_p$.

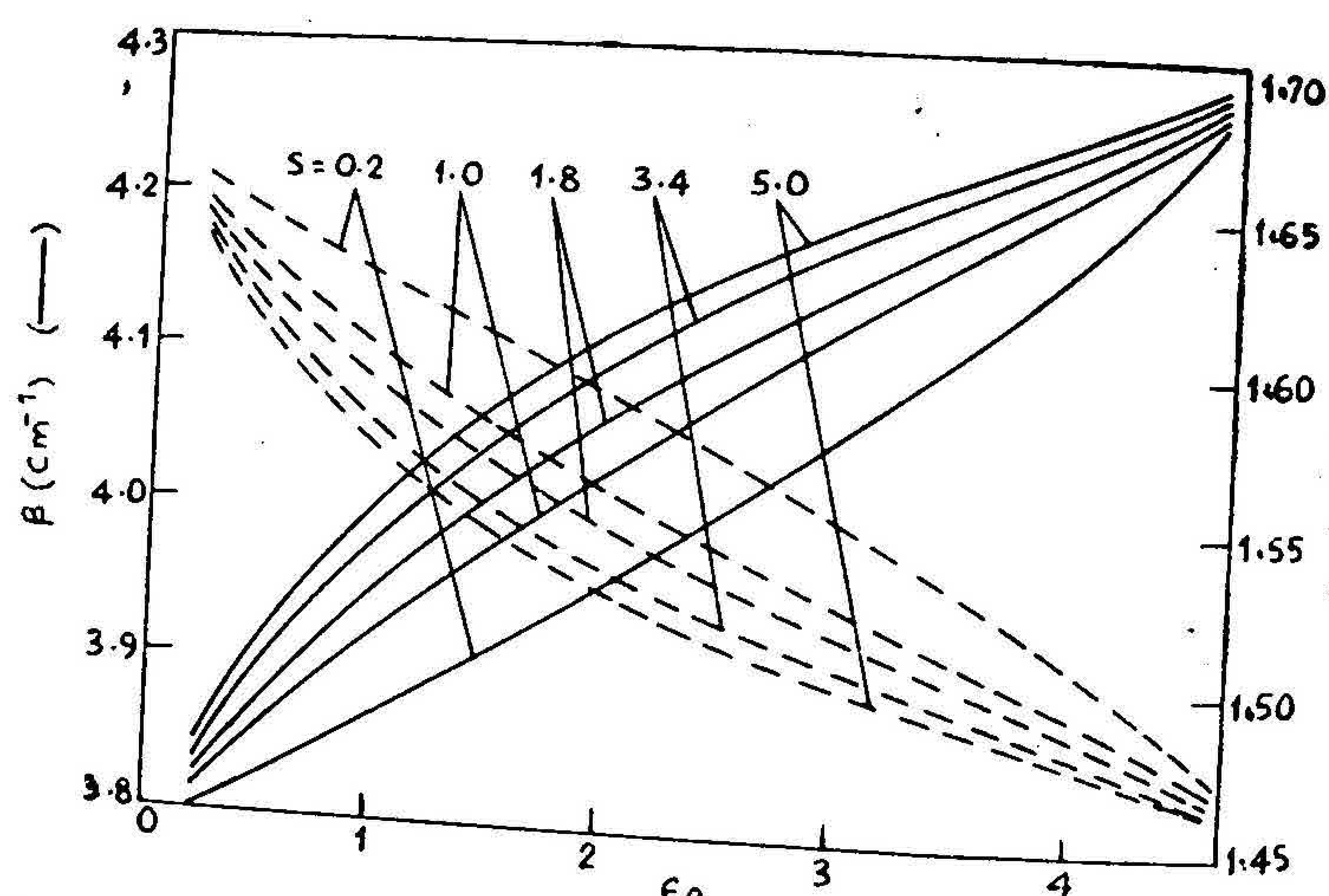

FIG. 24. Variation of β and λ_g with ϵ_p
$r_1 = 0 \cdot 1$ cm, $r_2 = 0 \cdot 12$ cm, $r_3 = 0 \cdot 62$ cm, $\epsilon_1 = 5 \cdot 0$, $\epsilon_3 = 4 \cdot 8$, $s = \epsilon_s/\epsilon_p$.

where

$$a_1^2 + a_3^2\left(\frac{\epsilon_\rho}{\epsilon_z}\right) = k_0^2(\epsilon_1 - \epsilon_3)$$

and

$$a_2^2 + a_3^2\left(\frac{\epsilon_\rho}{\epsilon_z}\right) = k_0^2(\epsilon_2 - \epsilon_3) \tag{46 a}$$

(ii) Dielectric-coated cconductor, coated with a graded dielectric

$$\left[\frac{\epsilon_z}{a_3} K_1(a_3r_3)\, S_2(r_3) - X(r_3)\, K_0(a_3r_3)\, S_4(r_3)\right]$$

$$\times \left[[X(r_2)\, S_3(r_2)\, F_{00}(a_1r_2) + \frac{\epsilon_1}{a_1} S_1(r_2)\, F_{10}(a_1r_2)\right]$$

$$-\left[\frac{\epsilon_z}{a_3} \cdot K_1(a_3r_3)\, S_1(r_3) - X(r_3)\, K_0(a_3r_3)\, S_3(r_3)\right]$$

$$\times \left[\chi(r_2)\, S_4(r_2)\, F_{00}(a_1r_2) + \frac{\epsilon_1}{a_1} S_2(r_2)\, F_{10}(a_1r_2)\right] \tag{47}$$

where

$$a_1^2 + a_3^2\left(\frac{\epsilon_\rho}{\epsilon_z}\right) = k_0^2(\epsilon_1 - \epsilon_3)$$

and

$$a_2^2(\rho) + a_3^2\left(\frac{\epsilon_\rho}{\epsilon_z}\right) = k_0^2\, \epsilon_2(\rho) - \epsilon_3. \tag{47 a}$$

(iii) Conductor coated with two graded dielectrics

$$\left[\frac{\epsilon_z}{a_3} K_1(a_3r_3)\, S_2(r_3) - X(r_3)\, K_0(a_3r_3)\, S_4(r_3)\right]$$

$$\times [\chi(r_2)\, S_3(r_2)\, P_0(r_2) - Y(r_2)\, S_1(r_2)\, P_1(r_2)]$$

$$-\left[\frac{\epsilon_z}{a_3} K_1(a_3r_3)\, S_1(r_3) - X(r_3)\, K_0(a_3\, r_3)\, S_3(r_3)\right]$$

$$\times [X(r_2)\, S_0(r_2)\, P_0(r_2) - Y(r_2)\, S_2(r_2)\, P_1(r_2)] \tag{48}$$

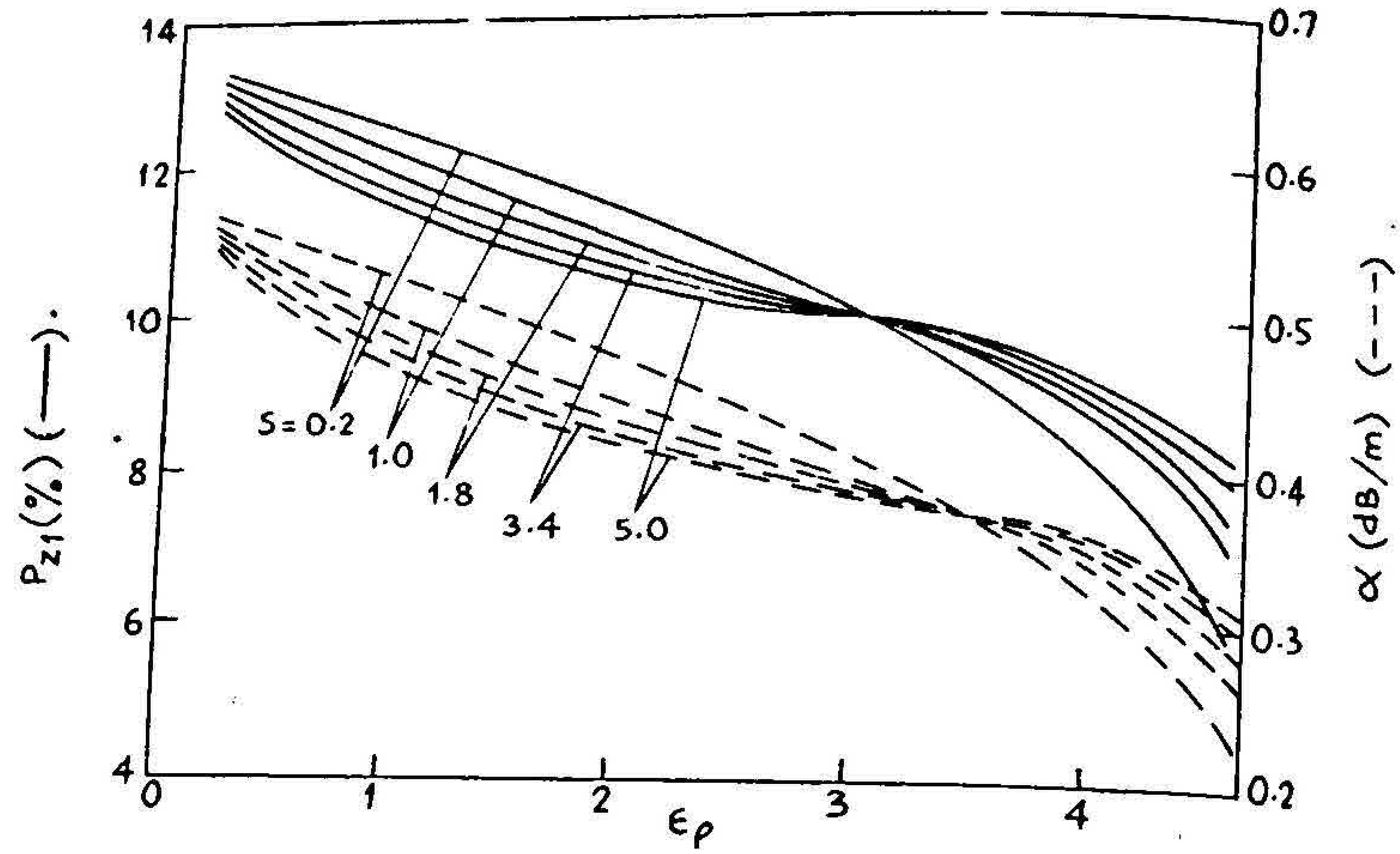

FIG. 25. Variation of P_{z1} and α with ϵ_p
$r_1 = 0{\cdot}1$ cm, $r_2 = 0{\cdot}12$ cm, $r_3 = 0{\cdot}62$ cm, $\epsilon_1 = 5{\cdot}0$, $\epsilon_2 = 4{\cdot}8$, $s = \epsilon_s/\epsilon_p$.

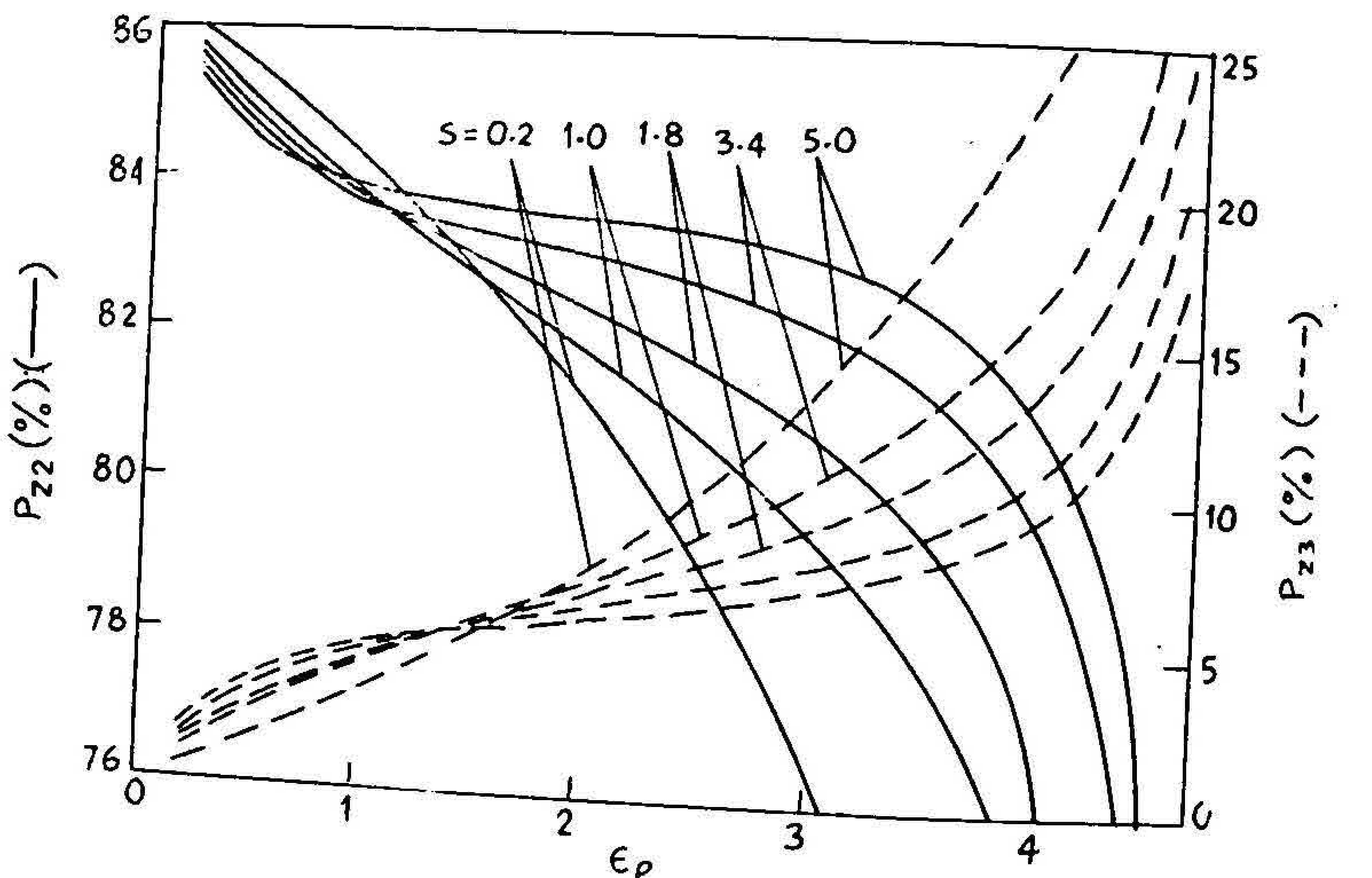

FIG. 26. Variation of P_{z2} and P_{z3} with ϵ_p
$r_1 = 0{\cdot}1$ cm, $r_2 = 0{\cdot}12$ cm, $r_3 = 0{\cdot}62$ cm, $\epsilon_1 = 5{\cdot}0$, $\epsilon_2 = 4{\cdot}8$, $s = \epsilon_s/\epsilon_p$

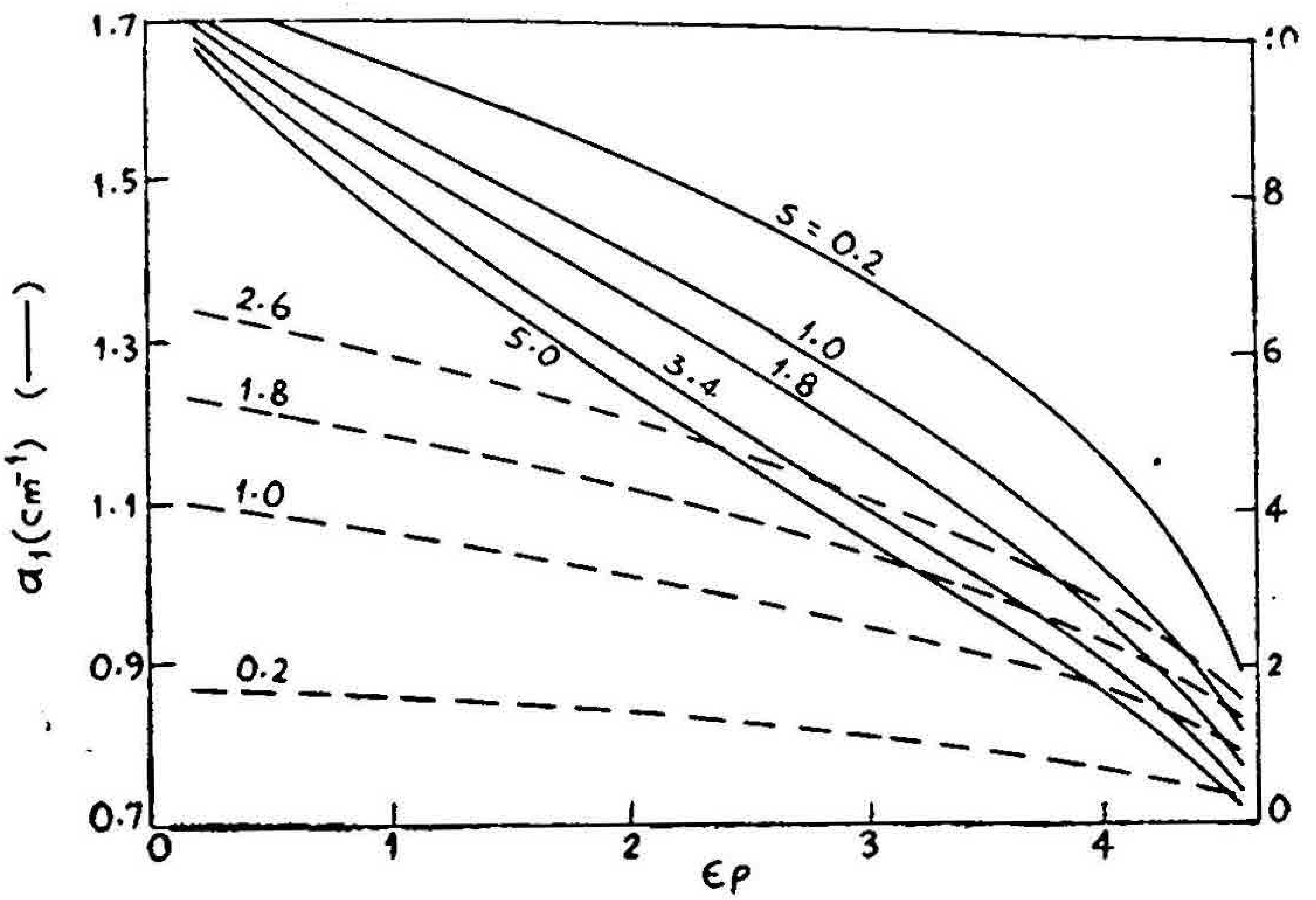

FIG. 27. Variation of a_1 and a_3 with ϵ_p
$r_1 = 0 \cdot 1$ cm, $r_2 = 0 \cdot 12$ cm, $r_3 = 0 \cdot 72$ cm, $\epsilon_1 = 5 \cdot 0$, $d = 0 \cdot 2\,cm^{-1}$.
Profile : Quadratic (single graded).

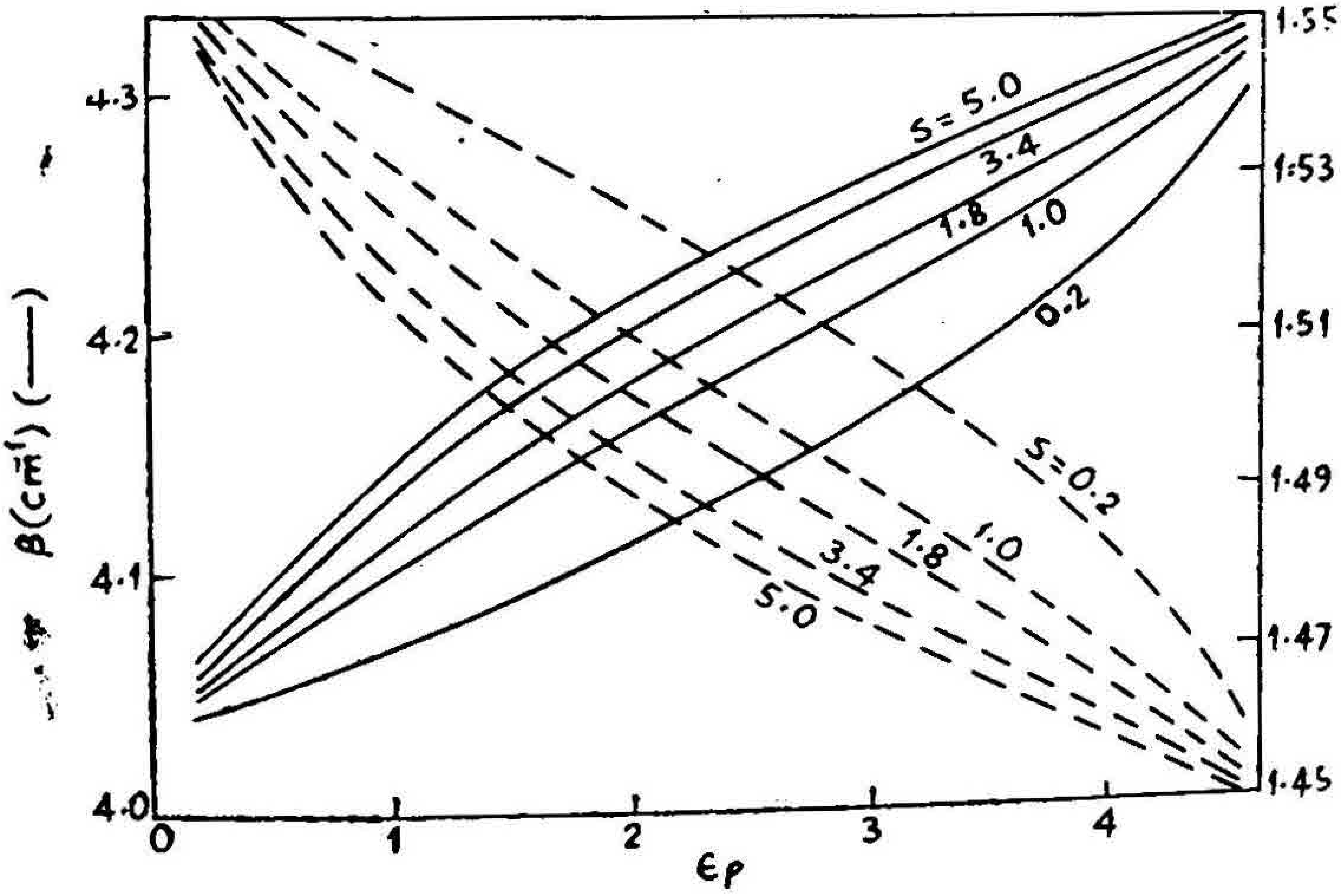

FIG. 28. Variation of β and λ_g with ϵ_p
$r_1 = 0 \cdot 1$ cm, $r_2 = 0 \cdot 12$ cm, $r_3 = 0 \cdot 72$ cm, $\epsilon_1 = 5 \cdot 0$, $d = 0 \cdot 2\,cm^{-1}$.
Profile : Quadratic (single-graded).

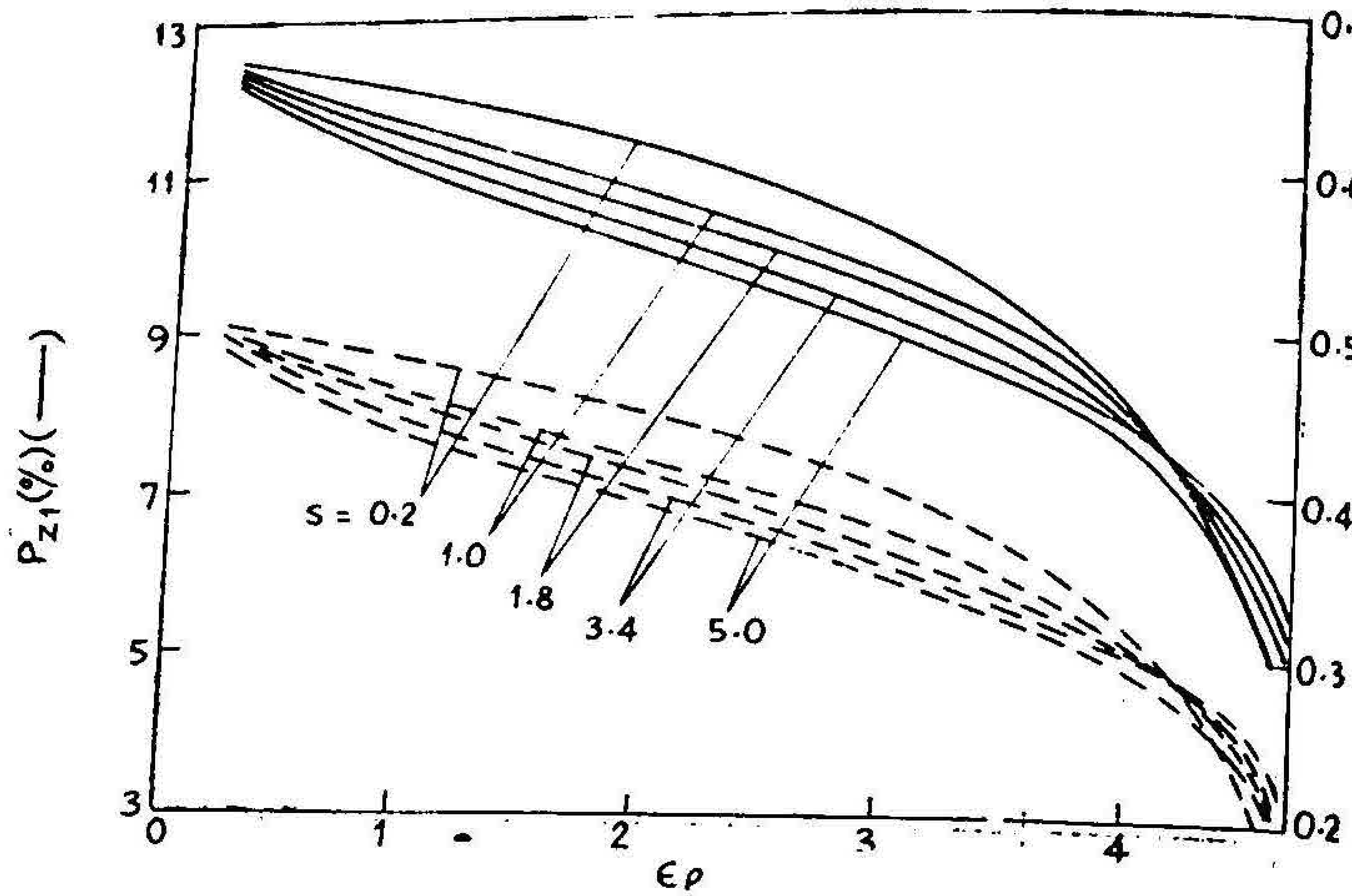

FIG. 29. Variation of P_{z1} and α with ϵ_ρ
$r_1 = 0{\cdot}1$ cm, $r_2 = 0{\cdot}12$ cm, $r_3 = 0{\cdot}72$ cm, $d = 0{\cdot}2$ cm^{-1}.
Profile : Quadratic (single-graded).

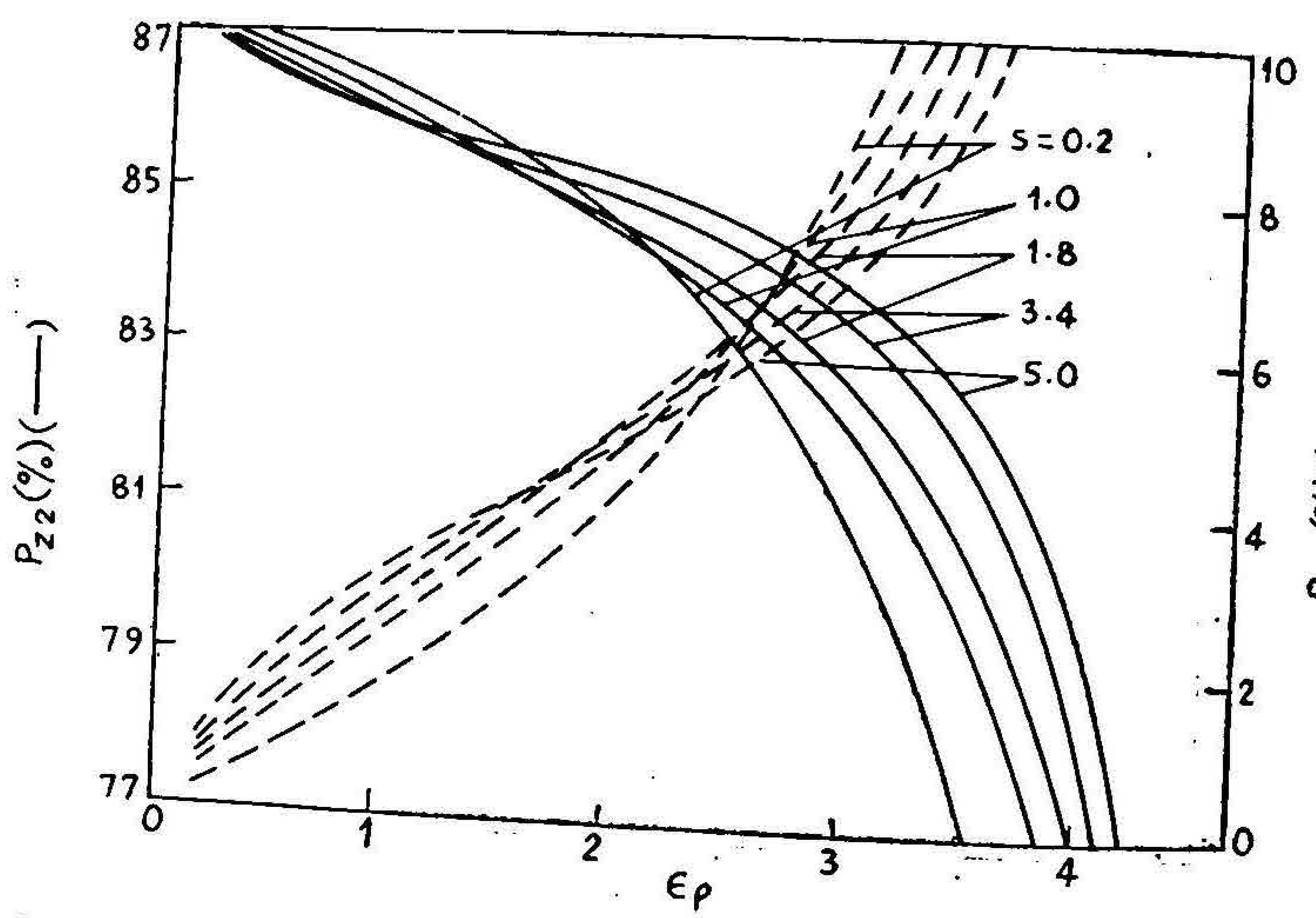

FIG. 30. Variation of P_{z2} and P_{z3} with ϵ_ρ
$r_1 = 0{\cdot}1$ cm, $r_2 = 0{\cdot}12$ cm, $r_3 = 0{\cdot}72$ cm, $d = 0{\cdot}2$ cm^{-1}.
Profile : Quadratic (single-graded).

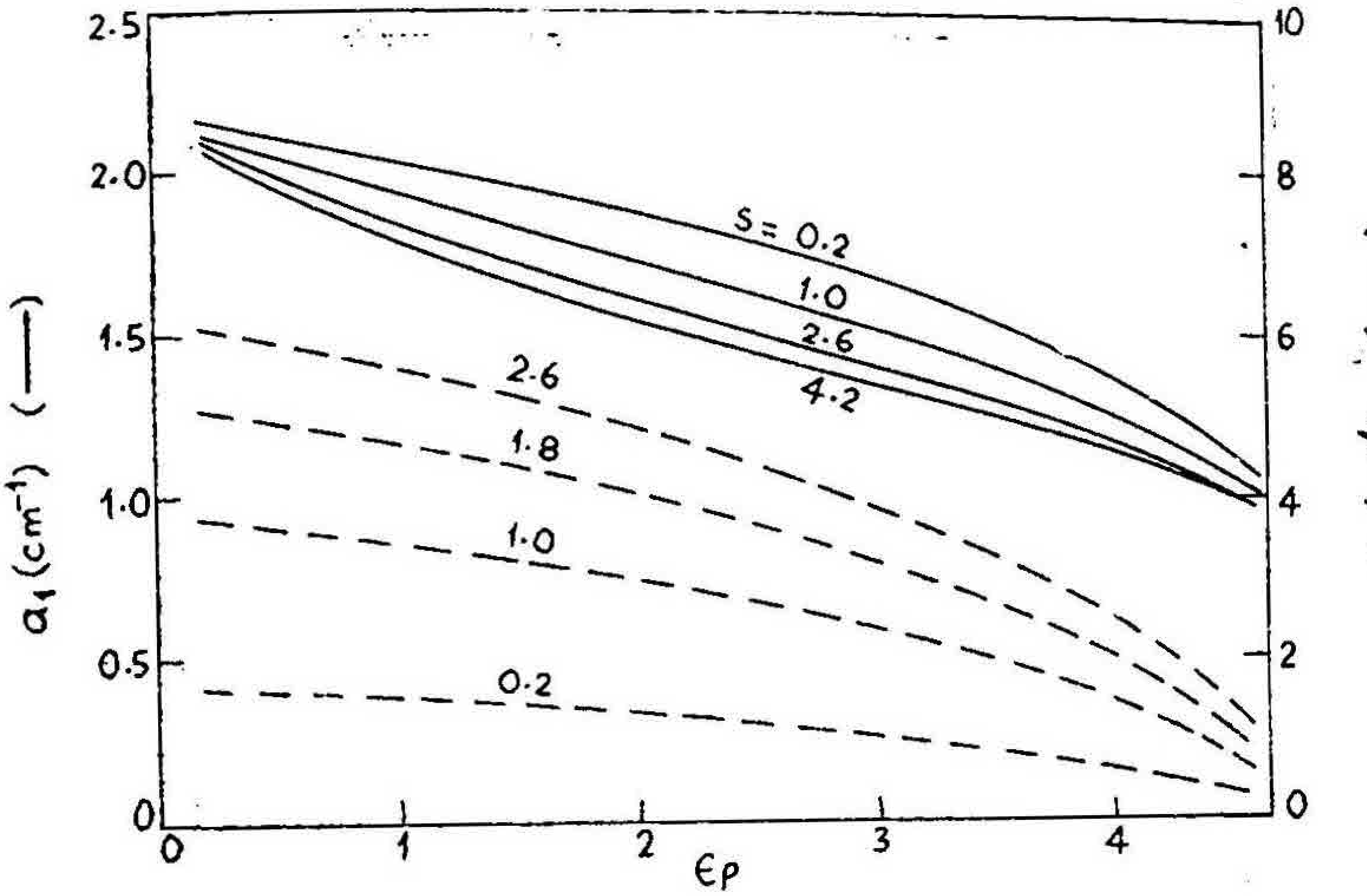

FIG. 31. Variation of a_1 and a_3 with ϵ_p
$r_1 = 0 \cdot 1$ cm, $r_2 = 0 \cdot 12$ cm, $r_3 = 0 \cdot 62$ cm, $\epsilon_1 = 5 \cdot 0$, $d = 0 \cdot 4\,\text{cm}^{-1}$.
Profiles : Quadratic (doubly-graded).

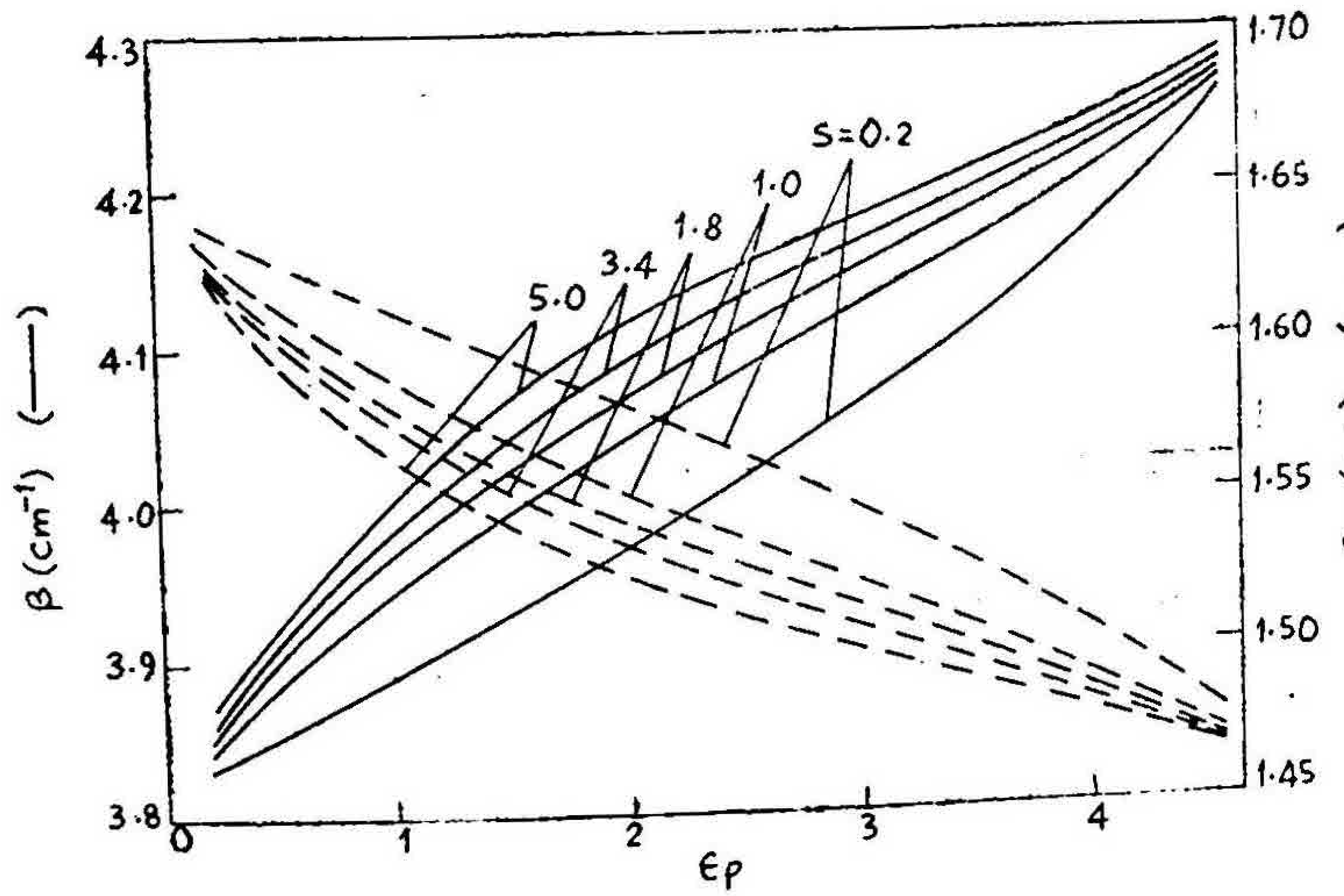

FIG. 32. Variation of β and λ_g with ϵ_p
$r_1 = 0 \cdot 1$ cm, $r_2 = 0 \cdot 12$ cm, $r_3 = 0 \cdot 62$ cm, $\epsilon_1 = 5 \cdot 0$, $d = 0 \cdot 4\,\text{cm}^{-1}$.
Profiles : Quadratic (doubly-graded).

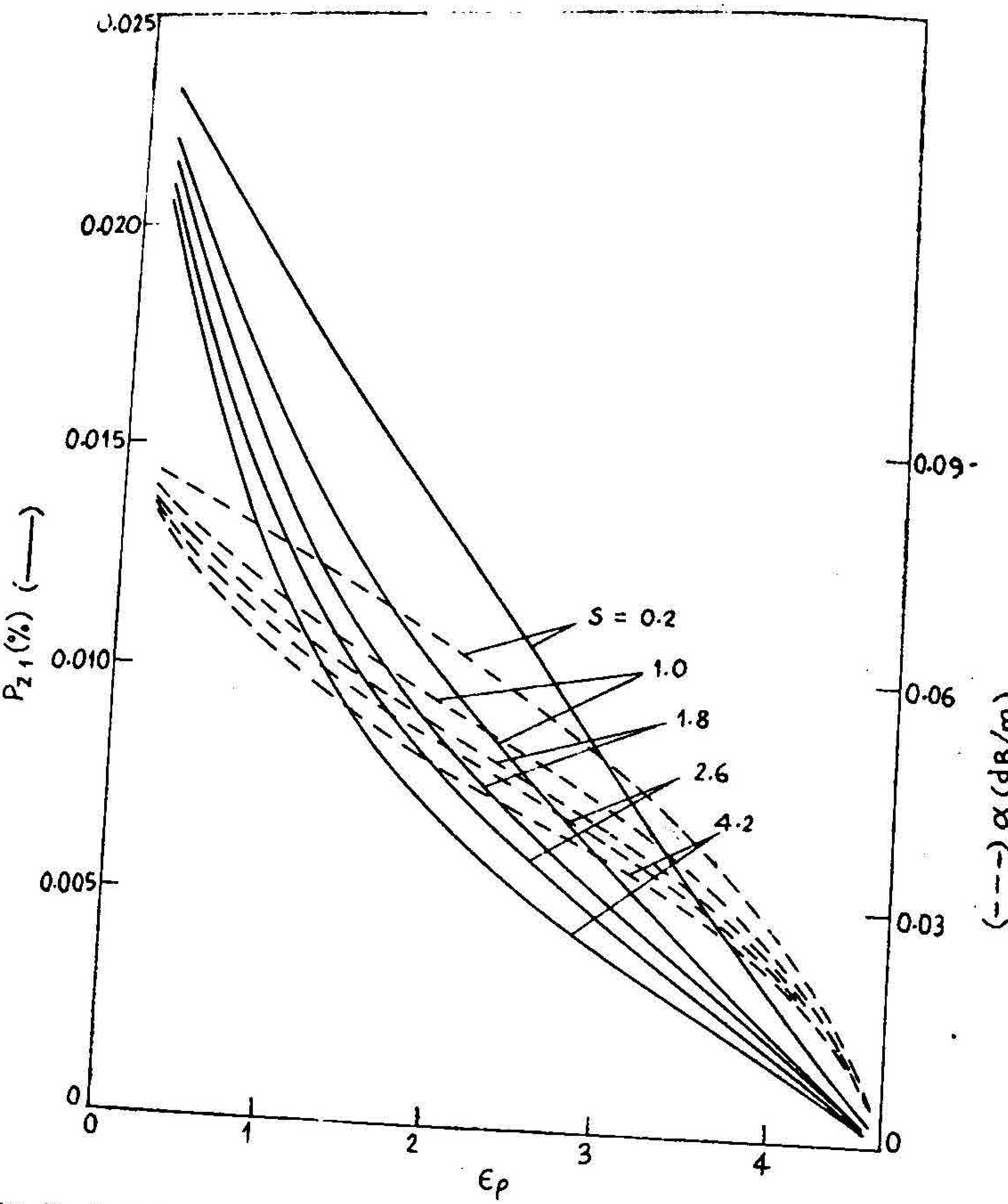

FIG. 33. Variation of P_{z1} and α with ϵ_ρ
$r_1 = 0 \cdot 1$ cm, $r_2 = 0 \cdot 12$ cm, $r_3 = 0 \cdot 7$ cm, $\epsilon_1 = 5 \cdot 0$, $d = 0 \cdot 4\,\text{cm}^{-1}$.
Profiles: Quadratic (doubly-graded).

where

$$a_1^2(\rho) + a_3^2\left(\frac{\epsilon_\rho}{\epsilon_z}\right) = k_0^2\,[\epsilon_1(\rho) - \epsilon_3)]$$

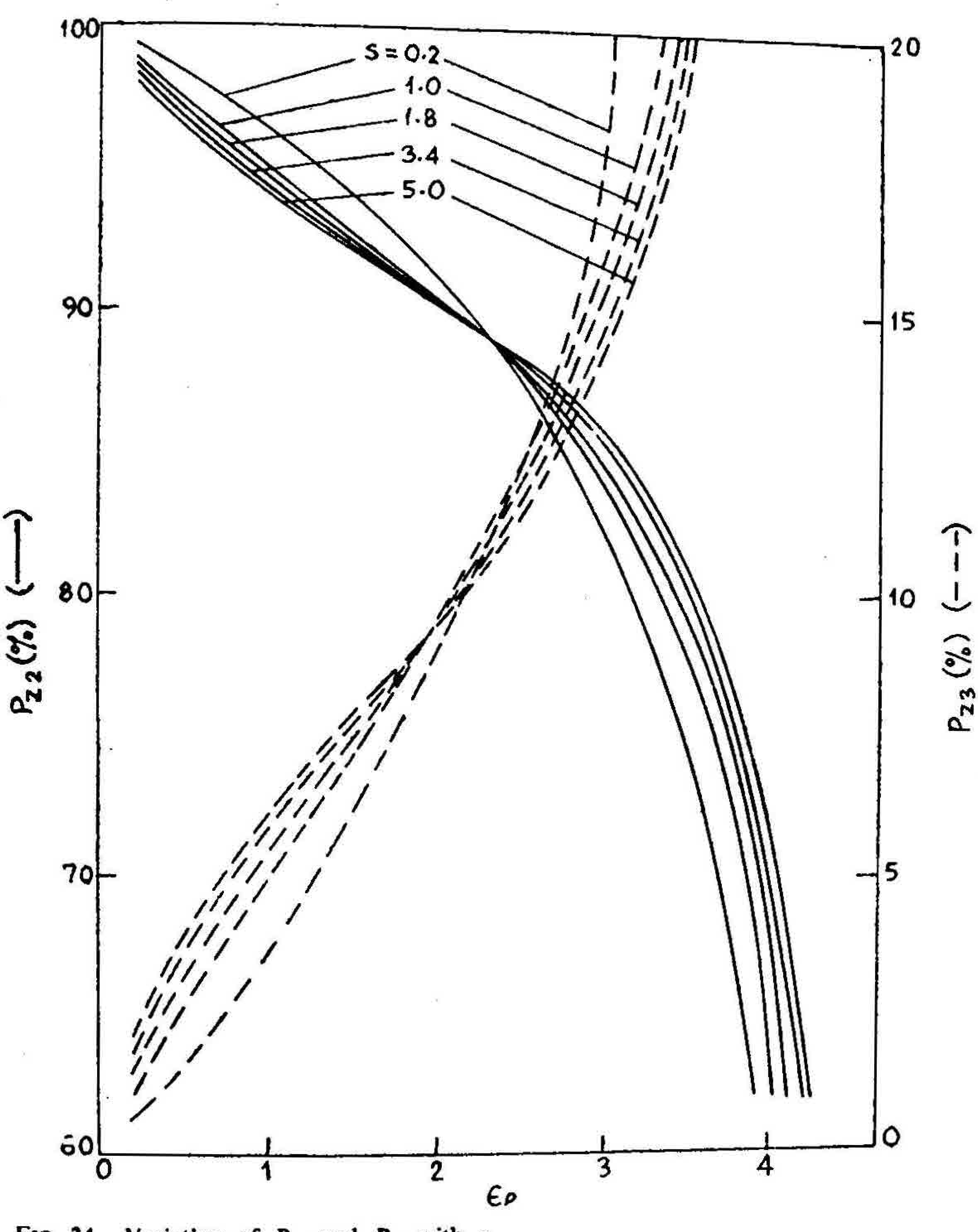

FIG. 34. Variation of P_{z2} and P_{z3} with ϵ_ρ
$r_1 = 0.1$ cm, $r_2 = 0.12$ cm, $r_3 = 0.62$ cm, $\epsilon_1 = 5.0$, $d = 0.4\,\text{cm}^{-1}$, $s = \epsilon_z/\epsilon_\rho$.
Profiles : Quadratic (doubly-graded).

and

$$a_2^2(\rho) + a_3^2\left(\frac{\epsilon_\rho}{\epsilon_z}\right) = k_0^2\,[\epsilon_2(\rho) - \epsilon_3] \tag{48 a}$$

$S_1(\rho)$, $S_2(\rho)$, $S_3(\rho)$ and $S_4(\rho)$ are the same as in previous sections.

The above three characteristic equations are solved to give the surface wave characteristics.

The power flowing in the external anisotropic medium for the three different cases is given by

$$P_{z3} = \frac{\pi\omega\epsilon_0\beta\epsilon_\rho}{2a_3^2}\left(\frac{\epsilon_z}{\epsilon_\rho}\right)^2 DD^* F(a_3r_3) \tag{49}$$

where $F(a_3r_3)$ is given by equation 20 *a*

The results of numerical computations are presented in Figs. 23-34. It may be concluded that the effect of the anisotropy factor $s\,(=\epsilon_z/\epsilon_\rho)$ is to

(i) cause a decrease in a_1 but increase in a_3

(ii) increase β and hence decrease λ_g

(iii) decrease P_{z1} and P_{z3} but increase P_{z2}

(iv) decrease the attenuation constant α.

16. CONCLUSIONS

The analysis of different cases leads to the main conclusion that by a proper choice of the profiles of multilayer delectric coating on a conductor, it may be possible to concentrate most of the power flow within the dielectrics It may be worthwhile to suggest that if the combination of profiles are so chosen that the microwave field extends neither to the central conductor nor up to the outside surface of the outermost dielectric coating, thus creatting the conditions of existence of an electric wall at the interface between the outermost surface of the structure and the external medium, then there may be a possibility of transmission of microwave power through a multi-dielectric coated cable.

REFERENCES

[1] Glory John, and Chatterjee, S. K. Effects of environmenta lon the surface wave characteristics of a dielectric-coated conductor—Part I, *Jour. of the Ind. Inst of Sci.*, 1974, 5, 80–103.

[2] Glory John, Chatterjee, R., a. d Chatterjee, S. K. Surface wave characteristics of a Lossy dielectric-coated conductor immersed in a lossy dielectric medium, *Proceedings I.E.E.—I..R.E.E.*, (India), 1974, 12, 210–227.

[3] Glory John, Chatterjee, R., and Chatterjee, S. K. Effects of environment on the surface wave characteristics of a dielectric-coated conductor—Part II, *Jour. of the Ind. Inst. of Sci.*, 1975, 57, 113–126.